

ORIGINAL ARTICLE

CD16⁺ CD56⁻ NK cells in the peripheral blood of cord blood transplant recipients: a unique subset of NK cells possibly associated with graft-versus-leukemia effectXuzhang Lu¹, Yukio Kondo¹, Hiroyuki Takamatsu¹, Kinya Ohata¹, Hirohito Yamazaki², Akiyoshi Takami³, Yoshiki Akatsuka⁴, Shinji Nakao¹¹Cellular Transplantation Biology, Kanazawa University Graduate School of Medical Science, Kanazawa, Ishikawa, Japan; ²The Protected Environmental Unit, Kanazawa University Hospital, Kanazawa, Ishikawa, Japan; ³Division of Transfusion Medicine, Kanazawa University Hospital, Kanazawa, Ishikawa, Japan; ⁴Division of Immunology, Aichi Cancer Research Institute, Nagoya, Aichi, Japan**Abstract**

A marked increase in CD16⁺ CD56⁻ NK cells in the peripheral blood (PB) was observed in a cord blood transplant (CBT) recipient with refractory acute myeloid leukaemia (AML) in association with attaining molecular remission. CD16⁺ CD56⁻ NK cells isolated from the patient became CD16⁺CD56⁺NKG2D⁺ when they were cultured in the presence of IL-2. Although cultured CD16⁺CD56⁻ NK cells retained the killer-cell immunoglobulin receptor (KIR)-ligand (KIR-L) specificity and the patient's leukemic cells expressed corresponding KIR ligands, they killed patient's leukemic cells expressing ULBP2. The cytotoxicity by cultured CD16⁺CD56⁻ NK cells was abrogated by anti-ULBP2 antibodies. When leukemic cells obtained at relapse after CBT were examined, both the ULBP2 expression and susceptibility to the cultured NK cells decreased in comparison to leukemic cells obtained before CBT. An increase in the CD16⁺CD56⁻ NK cell count ($0.5 \times 10^9/L$ or more) in PB was observed in seven of 11 (64%) CBT recipients but in none of 13 bone marrow (BM) and eight peripheral blood stem cell (PBSC) transplant recipients examined during the similar period after transplantation. These findings suggest an increase in CD16⁺CD56⁻ NK cells to be a phenomenon unique to CBT recipients and that mature NK cells derived from this NK cell subset may contribute to the killing of leukemic cells expressing NKG2D ligands *in vivo*.

Key words CD56⁺CD16⁻ NK cell; NKG2D; graft-versus-leukemia; cord blood transplantation**Correspondence** Shinji Nakao, Cellular Transplantation Biology, Kanazawa University Graduate School of Medical Science, Kanazawa University Hospital, 13-1 Takara-machi Kanazawa, Ishikawa 920-8640, Japan. Tel: +81-76-265-2274; Fax: +81-76-234-4252; e-mail: snakao@med3.m.kanazawa-u.ac.jp

Accepted for publication 6 March 2008

doi:10.1111/j.1600-0609.2008.01073.x

Cord blood transplantation (CBT) is being increasingly used for treatment of hematologic malignancies because its efficacy in the treatment of adult patients has been proven based on the findings of recent studies (1–4). One possible drawback of CBT is the less potent graft-versus-leukemia (GVL) effect than that of bone marrow transplantation (BMT) or peripheral blood stem cell transplantation (PBSCT) due to the immaturity of T cells contained in the cord blood (CB) graft (5). However, a recent study has shown the relapse rate after CBT to be comparable to that after BMT or PBSCT from human leukocyte antigen (HLA) matched sibling donors (1). Moreover, an analysis on the outcome of CBT for adult

patients with acute myeloid leukaemia (AML) in Japan revealed that the rate of leukemic relapse after HLA-mismatched CBT was lower than that after HLA-matched CBT despite the fact that the incidence of graft-versus-host disease (GVHD) was similar between the two groups (Cord Blood Bank Network of Japan; unpublished observation). These clinical findings suggest that immunocompetent cells other than T cells may mediate the GVL effect after CBT.

Natural killer (NK) cells play a major role in the development of GVL effect after an HLA-mismatched stem cell transplantation (SCT) (6, 7). The GVL effect by NK cells depends on the presence of

HLA-mismatches and T cell recovery after SCT (8). Because CBT is often carried out from HLA-mismatched donors and is also associated with delayed T cell recovery (9–11), NK cells may be more likely to contribute to the development of GVL effect after CBT than after BMT or PBSCT. Few studies, however, have previously focused on the GVL effect by NK cells after CBT.

CB has a unique subset of NK cells characterized by a phenotype CD16⁺CD56⁻ (12–14). This NK cell subset is thought to be immature NK cells capable of differentiating into CD16⁺CD56⁺ NK cells (15). We recently observed an apparent increase in this NK cell subset in a patient who underwent reduced-intensity CBT for the treatment of relapsed AML after PBSCT from an HLA-compatible sibling donor. The patient achieved a molecular remission of AML in association with the NK cell increase. This observation prompted the characterization of CD16⁺CD56⁻ NK cells of this patient and other patients after allogeneic SCT. The present study revealed that CD16⁺CD56⁻ NK cells may potentially play a role in the development of the GVL effect in patients whose leukemic cells express NKG2D ligands.

Materials and methods

Patients

Peripheral blood (PB) was obtained from 11 CBT, 13 BMT (10 from related and three from unrelated donors), and eight PBSCT patients 2–135 months after transplantation. None of the patients had active graft-versus-host disease requiring corticosteroids at time of sampling or signs of infection. The original diseases of the CBT recipients included AML in four, non-Hodgkin's lymphoma (NHL) in four, myelodysplastic syndromes (MDS) in two and renal cell carcinoma in one. In the BMT recipients, those were AML in four, acute lymphoblastic leukemia (ALL) in four, MDS in three, chronic myeloid leukaemia (CML) in one, and aplastic anaemia (AA) in one while in the PBSCT recipients, those were AML in four, ALL in one, biphenotypic leukemia in two and NHL in one. All CBT recipients received an HLA-mismatched graft; the number of HLA mismatches between donor and recipient were two in seven, three in three and four in one. No HLA mismatch was observed between each donor and the BMT or PBSCT recipient except for six PBSCT recipients whose mismatches with their donors was one in two, two in one and three in one. This study was approved by our institutional review board and all patients gave their informed consent for the phenotypic and functional analyses of their peripheral blood mononuclear cells (PBMCs).

Phenotype analysis of PBMC after SCT and leukemia cells

The cell surface phenotype was determined by three-color flow cytometry. The cells were stained with various monoclonal antibodies (mAbs) specific to cell surface proteins including CD3, CD56, CD16, CD158a, CD158b (Becton Dickinson Pharmingen), NKG2A, NKG2D, NKp30, NKp44 and NKp46 (Beckman Coulter, Marseille, France). The expression of NKG2D ligands on leukemic cells from a CBT recipient was determined using mAbs specific to MICA/B (Becton Dickinson Pharmingen), ULBP1, ULBP2 and ULBP3 (R&D Systems, Minneapolis, MN).

Cell separation

PBMCs were isolated using density gradient centrifugation. NK cells were enriched by negative selection using immunomagnetic beads (DynaL NK cell isolation kit; Dynal Biotech, Lake success, NY) according to the manufacturer's recommendation (16). NK cell purity was confirmed by flow cytometry. CD16⁺CD56⁺ and CD16⁺CD56⁻ NK cells were separated from the enriched NK cells with anti-CD56-coated microBeads (MACS) by passing them through two sequential large-scale columns (Milteny Biotec, Gladbach, Germany) according to the manufacturer's instructions. CD158b⁺ and CD158b⁻ NK cells were separated with anti-CD158b-FITC Abs and anti-FITC microbeads.

NK cell culture

Isolated 2×10^6 CD16⁺CD56⁺ and CD16⁺CD56⁻ subsets were cultured with or without 2×10^5 irradiated (45 Gy) K562 cells transfected with the membrane-bound form of IL-15 and human 4-1BBL (K562-mb15-41BBL) kindly provided by Dr. Dario Campana of University of Tennessee College of Medicine (17) in RPMI1640 containing 10% fetal bovine serum (FBS), 50 U/mL penicillin, 50 µg/mL streptomycin and 100 IU/mL IL-2 for 14 d. The cultured NK cells were washed with RPMI1640 and then were used for the cytotoxicity assay.

Transfection of 721-221 cells with retroviral vector

An HLA class I-negative B cell line 721–221 was transfected with retrovirus vectors containing HLA-C*0301 (.221-Cw3) or HLA-C*0401 (.221-Cw4) as described previously (18). Transfectants were selected in the presence of 0.1 mg/mL neomycin and 0.1 mg/mL puromycin. The surface expression of HLA-C molecules was confirmed by flow cytometry using a mAb HLA-ABC (Immuno- tech, Marseille, France). A clone exhibiting the highest

level of HLA-C expression was used as a target in the cytotoxicity assay.

Cytotoxicity assay

NK cell cytotoxicity was assessed using the standard chromium release assay, as described previously (19). In blocking experiments, anti-ULBP Abs were added at 10 µg/mL to the ⁵¹Cr labeled target cells and target cells were incubated at 37°C for 30 min before the addition of NK cells. The percentage of specific lysis was calculated using the formula: $100 \times (\text{count per minute [cpm]} \text{ released from test sample} - \text{cpm spontaneous release}) / (\text{cpm maximum release} - \text{cpm spontaneous release})$.

Statistical analysis

The significance of difference in the PB CD16⁺CD56⁻ cell count between CBT recipients and recipients of BM, PBSCT, or healthy individual was assessed by Student's *t*-test. The significance of difference in the time of sampling after SCT between CBT, BMT and PBSCT was assessed by Mann-Whitney test. *P*-values <0.05 were considered to be significant.

Results

An increase in the number of CD16⁺CD56⁻ NK cells in a CBT recipient

A 56-yr-old male (Patient 1) who relapsed with AML M0 after PBSCT from a sibling donor underwent CBT following preconditioning with fludarabine 125 mg/m², melphalan 80 mg/m², and 4 Gy TBI. The patient's leukemia was refractory to chemotherapy and there were 18% leukemic blasts in the PB at the time of preconditioning. He achieved complete chimerism in PB on day 22 after CBT. The WT1 copy number in BM RNA decreased from 13 000 copies/µg RNA before the start of preconditioning to 140 copies/µg RNA on day 60 (20). However, it rose to 1500 copies/µg RNA on day 80 after CBT. Although a molecular relapse was suspected, the WT1 copy number spontaneously decreased to 230 on day 172. Surface phenotype analysis of PB leukocytes on day 84 showed an increase in the count of CD3⁻CD16⁺CD56⁻ NK cells (Fig. 1). The CD16⁺CD56⁻ NK cell count remained as high as $3.2\text{--}4.5 \times 10^9/\text{L}$ for the following 11 months during which he remained in remission. The patient eventually relapsed with AML and died 16 months after CBT. The unexpected long term remission after reduced-intensity CBT associated with an increase in the CD16⁺CD56⁻ NK cell count prompted the characterization of the CD16⁺CD56⁻ NK cells of this patient and other patients who underwent allogeneic SCT.

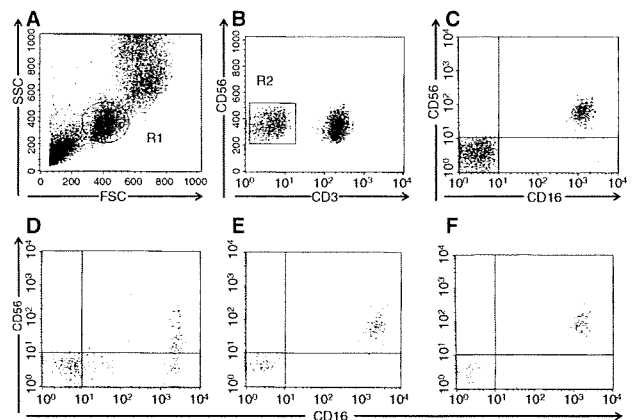


Figure 1 Phenotype of the CD16⁺ NK cells in the peripheral blood. Representative results of flow cytometry on CD3⁻ lymphocytes from SCT recipients and healthy individuals are shown. Gates were set up to exclude any CD3⁺ lymphocytes as shown in (A) and (B); (C) a healthy individual; (D) a CBT recipient (Patient 1); (E) a BMT recipient; (F) a PBSCT recipient.

CD16⁺CD56⁻ NK cells in PB of allogeneic SCT recipients

Because the presence of CD16⁺CD56⁻ NK cells has been reported to be characteristics of CB, the proportion of PB CD16⁺CD56⁻ NK cells as well as their absolute count was determined for other recipients of CB and the other stem cell grafts. An increase in the CD16⁺CD56⁻ NK cell count greater than $0.5 \times 10^9/\text{L}$ was seen in seven of 11 CBT recipients but in none of 13 BMT and eight PBSCT recipients (Figs 1 and 2). There was no significant difference in the time of sampling after SCT between CBT recipients and BMT recipients ($P > 0.772$) or CBT recipients and PBSCT recipients ($P > 0.265$). Both the CD16⁺CD56⁻ NK cell proportion and the absolute count were significantly higher in CBT recipients than in other SCT recipients or in healthy individuals. In contrast, there were no significant differences in the count of other NK cell subsets including CD56^{dim}CD16⁺ and CD56^{bright}CD16⁻ cells among these three SCT recipient groups (data not shown). A CD16⁺CD56⁻ NK cell increase greater than $1.5 \times 10^9/\text{L}$ was restricted to Patient 1 and another CBT recipient with NHL (Patient 2). The CD16⁺CD56⁻ NK cell counts of Patient 2, 5 months and 15 months after CBT were $1.5 \times 10^9/\text{L}$ and $1.8 \times 10^9/\text{L}$, respectively.

Surface phenotype of CD16⁺CD56⁻ NK cells and leukemic cells

To characterize this unusual NK cell subset, the surface phenotype was compared between CD16⁺CD56⁻ and CD16⁺CD56⁺ NK cells from Patient 1 and Patient 2

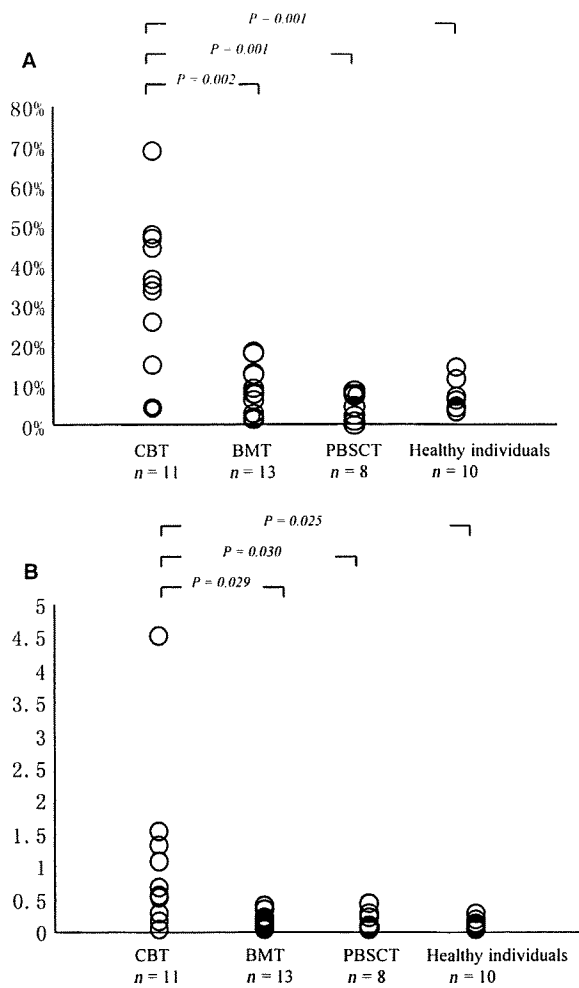


Figure 2 The proportion (A) and the absolute count (B) of CD3⁻CD16⁺CD56⁻ in the PB of SCT recipients and healthy individuals. An increase in the proportion of CD3⁻CD16⁺CD56⁻ NK cells (20% or more) in the PB CD16⁺ NK cells and an increase in the absolute count of the same NK cell subset (>0.5 × 10⁹/L) were observed in seven of 11 CBT recipients, but in none of allogeneic 13 BM and eight PBSC transplant recipients. The CD3⁻CD16⁺CD56⁻ cell count was calculated by multiplying the WBC count with the proportion (%) of this subset among the total cell event.

Table 1 Phenotype of the NK cell subsets from two CBT recipients

			NKp30		NKp44		NKp46		NKG2D	
			%	MFI	%	MFI	%	MFI	%	MFI
Patient 1	CD56 ⁺ CD16 ⁺	Fresh	3.7	11.5	0	7.51	56.7	37.9	61.0	35.6
		Cultured	43.1	33.2	71.2	88.9	61.3	48.1	100.0	156.0
	CD56 ⁺ CD16 ⁻	Fresh	0.0	8.37	0.0	7.57	17.6	12.6	46.7	12.6
		Cultured	14.2	10.4	51.4	31.0	54.2	26.8	99.9	26.8
Patient 2	CD56 ⁺ CD16 ⁺	Fresh	3.6	6.71	0.0	7.72	42.9	44.3	72.3	44.3
		Cultured	14.2	39.4	51.4	49.4	54.2	54.4	99.5	54.4
	CD56 ⁺ CD16 ⁻	Fresh	0.0	8.65	0.0	8.31	21.5	16.9	69.0	16.9
		Cultured	58.1	47.6	66.3	51.4	75.2	64.8	98.5	64.8

CD16⁺CD56⁻ and CD16⁺CD56⁺ NK cells were isolated from two CBT recipients and cultured with irradiated K562-mb15-41BBL in the presence of IL-2 for 14 d. Cultured NK showed increased expression of activating NK receptors including NKp30, NKp44, NKp46 and NKG2D.

(Table 1). All CD16⁺CD56⁻ cells, similarly to CD16⁺CD56⁺ cells, expressed CD11a, CD18, but did not express a B-cell marker CD19, or the myeloid marker CD33 (data not shown). There were no differences in the expression levels of two major inhibitory NK receptors CD158a and CD158b between the two NK cell subsets (data not shown). On the other hand, the proportions of cells expressing activating NK receptors including NKG2D in CD16⁺CD56⁻ NK cells tended to be lower than those of CD16⁺CD56⁺ NK cells.

The leukemic cells obtained from Patient 1 before CBT exhibited an NKG2D ligand ULBP2 (Fig. 3). When the leukemic cells obtained after relapse was examined, the ULBP2 expression was observed to have decreased to levels comparable to ULBP1 and ULBP3.

Phenotypic change of CD16⁺CD56⁻ NK cells after *in vitro* culture

CD16⁺CD56⁻ NK cells derived from CB are reported to undergo differentiation *in vitro* in the presence of IL-2 (15, 21) and are therefore thought to be precursors of CD16⁺CD56⁺ NK cells (15). CD16⁺CD56⁻ NK cells were enriched from PBMCs of Patient 1 and Patient 2 and cultured in the presence of 100 IU/ml of IL-2 with or without irradiated K562-mb15-41BBL. In accordance with the results of previous studies, CD16⁺CD56⁻ NK cells from Patient 1 became CD16⁺CD56⁺ after *in vitro* culture (Fig. 4). Cultured CD16⁺CD56⁻ NK showed a tendency toward an increased expression of activating receptors including NKp30, NKp44, NKp46 and NKG2D, but did not show any changes in the expression of inhibitory receptors including CD158a, CD158b and NKG2A (Table 1).

Specificity of cultured CD16⁺CD56⁻ NK cells

Although attaining molecular remission in association with an increase in the CD16⁺CD56⁻ NK cells suggests the involvement of these NK cells in the GVL effect,

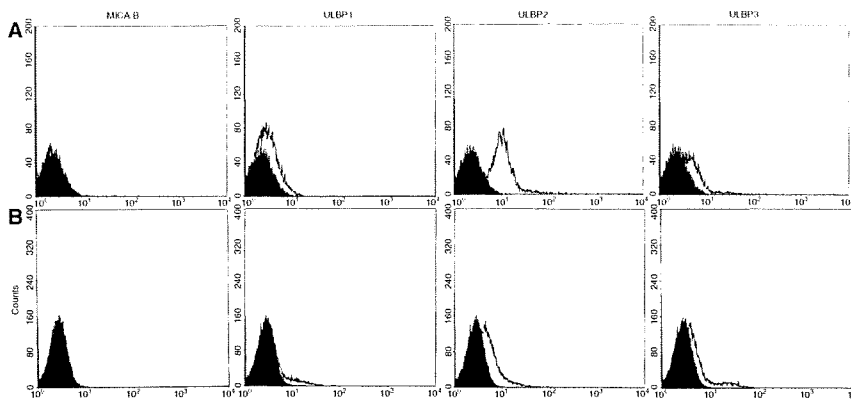


Figure 3 Expression of NKG2D ligands on leukemic cells from Patient 1. (A) leukemic cells obtained before CBT; (B) leukemic cells obtained after relapse. The proportion of ULBP2 expressing leukemic cells decreased from 59% to 9%.

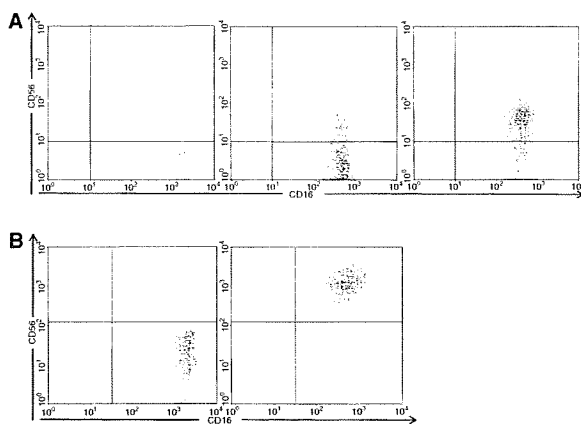


Figure 4 Phenotypic change of CD16⁺CD56⁻ NK cells with time associated with *in vitro* culture. Isolated CD16⁺CD56⁻ cells from Patient 1 were cultured in the presence of 100 IU/L IL-2 without (A) or with K562-mb15-41BBL (B). CD16⁺CD56⁻ NK cells from CBT recipients became CD16⁺CD56⁺ after the *in vitro* culture.

there was no killer-cell immunoglobulin receptor (KIR)-ligand (KIR-L) mismatch between Patient 1 and the CB donor; Patient 1 and the CB donor shared C*0102 and

C*0304. To determine whether cultured NK cells derived from CD16⁺CD56⁻ NK cells retain specificity restricted by KIR-L of target cells, cultured NK cells from Patient 1 and Patient 2 who possessed C*0102 and C*1202 were separated into CD158b⁺ and CD158b⁻ NK cells, and were examined for their cytotoxicity against 721-221 cells transfected with different HLA-C alleles (Fig. 5). CD158b⁺ NK cells failed to kill 721-221 cells transfected with HLA-C*0301 (.221-Cw3) while they killed both wild-type 721-221 cells and 721-221 cells transfected with HLA-C*0401 (.221-Cw4). Conversely, CD158b⁻ NK cells not only killed 721-221 cells but they also killed .221-Cw3 and .221-Cw4 cells, thus indicating that the cytotoxicity due to the cultured CD158b⁺ NK cells is inhibited by the KIR-L Cw3 of the target cells.

Cytotoxicity of cultured CD16⁺CD56⁻ NK cells against leukemic cells

When leukemic cells obtained from Patient 1 before CBT were used as a target, both CD158b⁺ and CD158b⁻ NK cells showed similar cytotoxicity to that of unfractionated NK cells (Fig. 6). The cytotoxicity was blocked by

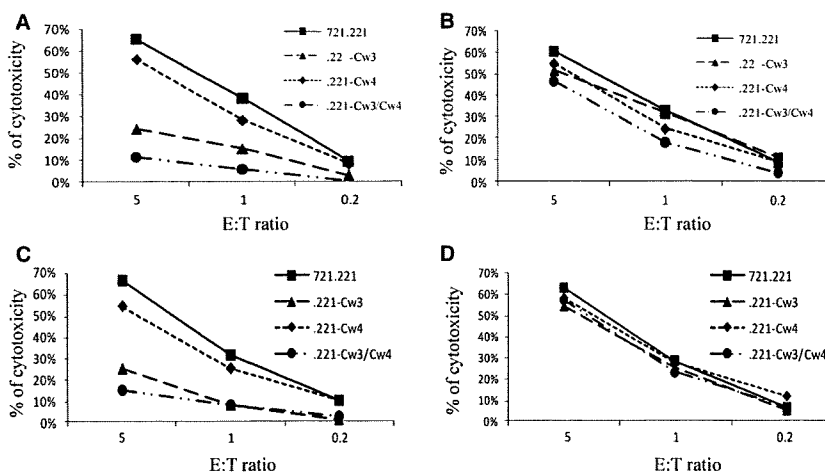


Figure 5 Specificity of NK cells derived from CD16⁺CD56⁻ NK cells. Cultured NK cells derived from CD16⁺CD56⁻ cells of Patient 1 (A and B) and Patient 2 (C and D) were separated into CD158b⁺ (A and C) and CD158b⁻ cells (B and D) and were examined for the cytotoxicity against 721-221 cells and 721-221 transfected with different HLA-C alleles C*0301 (.221-Cw3) and C*0401 (.221-Cw4). The data represent one of two experiments which produced similar results.

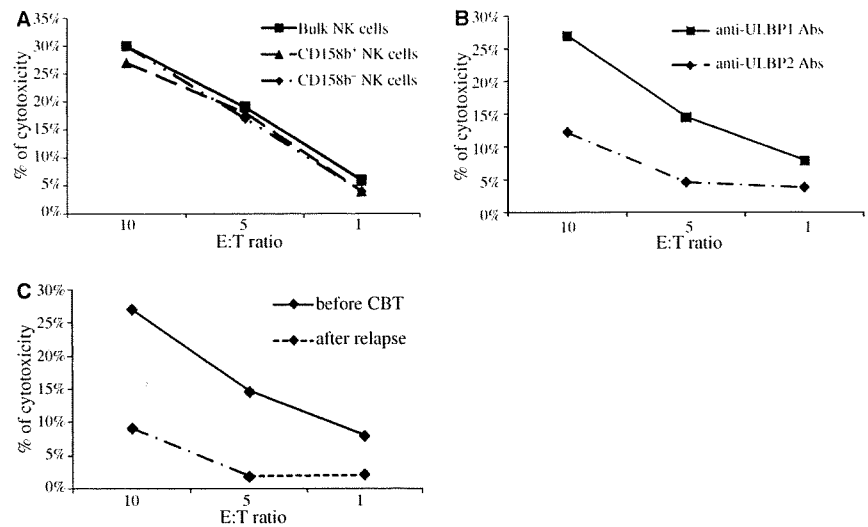


Figure 6 Cytotoxicity of cultured NK cells against leukemic cells. (A) Unseparated and separated NK cells were tested against leukemic cells obtained before CBT; (B) Leukemic cells were incubated in the presence of anti-ULBP1 or ULBP2 Abs before incubation with cultured NK cells; (C) Cytotoxicity of unseparated NK cells were tested against leukemic cells obtained before CBT or after relapse. The data represent one of three experiments which produced similar results.

treatment of leukemia cells with anti-ULBP2 mAbs. Leukemic cells obtained after relapse were relatively resistant to killing by cultured NK cells in comparison to those obtained before CBT.

Discussion

The present study revealed an increase in a unique NK cell subset characterized by CD16⁺CD56⁻ in CBT recipients. Although CD3⁻CD16⁺CD56⁻ cells comprise monocytes, an increase in this subset was due to an increase in immature NK cells because they did not express a myeloid marker CD33 and acquired CD56 expression by *in vitro* culture in the presence of IL-2. An increase in NK cells with a similar phenotype has been shown in patients with solid tumors who were treated with IL-2 (21) and in those with HIV infection (22). Our CBT recipients did not receive cytokine therapy nor show any signs of viral infections at sampling. The expression of KIRs including CD158a and CD158b was not depressed in CD16⁺CD56⁻ cells of Patient 1 and Patient 2 in contrast to those of HIV patients (22). An *in vitro* culture of CD16⁺CD56⁻ NK cells from patients with HIV viremia in the presence IL-2 reportedly failed to induce NKp44 expression while it did induce the NKp44 expression by CD16⁺CD56⁻ NK cells from the two CBT recipients. It is therefore unlikely that the increase in the CD16⁺CD56⁻ cell count in the CBT recipients was secondary to viral infections.

Gaddy *et al.* demonstrated a novel subset of NK cells characterized by a phenotype CD16⁺CD56⁻ to exist in CB (12). They hypothesized that this NK cell subset represents immature NK cells capable of differentiating into CD16⁺CD56⁺ NK cells (15). CD16⁺CD56⁻ cells of our

patients also underwent differentiation into CD16⁺CD56⁺ cells when they were cultured in the presence of IL-2. Therefore, CD16⁺CD56⁻ cells in PB after CBT may be derived from immature NK cells or NK precursor cells which existed in CB grafts. Previous studies on NK cells from SCT recipients and *ex vivo* engineered CB NK cells did not reveal an increased proportion of CD16⁺CD56⁻ cells (23–25). Both Patient 1 and Patient 2 received an HLA-mismatched CB graft although there was no KIR-L mismatch. Notably, Patient 1 had a large leukemic burden at the time of reduced-intensity preconditioning. It is therefore plausible that residual leukemic cells may have stimulated NK cell precursors to recruit CD16⁺CD56⁻ NK cells in Patient 1.

Patient 1's leukemic cells obtained before CBT expressed ULBP2. The incubation of CD16⁺CD56⁻ NK cells derived from Patient 1 in the presence of IL-2 and the K562 transfectant augmented NKG2D expression and the cultured NK cells showed cytotoxicity against leukemic cells despite that cultured NK cells retained KIR-L specificity and Patient 1's leukemic cells expressed matched KIR-L HLA-C*0304/C*0102. The cytotoxicity by the cultured NK cells decreased against leukemic cells treated with anti-ULBP2 Abs, and also against the leukemic cells obtained from Patient 1 after relapse which were devoid of ULBP2 expression. These findings suggest that mature NK cells derived from CD16⁺CD56⁻ NK cells may have exerted GVL effect on Patient 1's leukemic cells by way of interaction of NKG2D and ULBP2. The aberrant expression of NKG2D ligands by leukemic cells has been demonstrated by previous studies (26), but its influence on the outcome of allogeneic SCT has not yet been clarified. The results of the present study

indicate that the susceptibility of leukemic cells to NK cells may depend on both expression of NKG2D ligand on leukemic cells and the expression of NKG2D on effector NK cells. In patients with acute leukemia, leukemic cells are reported to downregulate NKp30 of autologous NK cells, thereby allowing NK cells to escape leukemic cells (27, 28). In the setting of CBT, leukemic cells expressing NKG2D ligands may tend to stimulate NK cell precursors in CB, thus inducing them to undergo differentiation.

The present study demonstrated the expansion of CD16⁺ CD56⁻ NK cells in the PB of CBT recipients for the first time. These immature NK cells can be expanded *ex vivo* with a help of K562-mb15-41BBL cells as maintaining specificity to KIR-L and cytotoxicity against leukemic cells expressing an NKG2D ligand. Therefore, CB may be a potential source of NK cells which can be utilized for cell therapy. Further studies on a larger number of CBT recipients are needed to determine whether CD16⁺ CD56⁻ NK cells indeed play a role in the GVL effect.

Acknowledgement

We thank Dr. Dario Campana and Dr Chihaya Imai for providing us with K562-mb15-41BBL cells.

References

1. Takahashi S, Ooi J, Tomonari A, *et al.* Comparative single-institute analysis of cord blood transplantation from unrelated donors with bone marrow or peripheral blood stem-cell transplants from related donors in adult patients with hematologic malignancies after myeloablative conditioning regimen. *Blood* 2007;**109**:1322–30.
2. Arcese W, Rocha V, Labopin M, *et al.* Unrelated cord blood transplants in adults with hematologic malignancies. *Haematologica* 2006;**91**:223–30.
3. Rocha V, Cornish J, Sievers EL, *et al.* Comparison of outcomes of unrelated bone marrow and umbilical cord blood transplants in children with acute leukemia. *Blood* 2001;**97**:2962–71.
4. Barker JN, Weisdorf DJ, DeFor TE, Blazar BR, McGlave PB, Miller JS, Verfaillie CM, Wagner JE. Transplantation of 2 partially HLA-matched umbilical cord blood units to enhance engraftment in adults with hematologic malignancy. *Blood* 2005;**105**:1343–7.
5. Harris DT, Schumacher MJ, Locascio J, Besencon FJ, Olson GB, DeLuca D, Shenker L, Bard J, Boyse EA. Phenotypic and functional immaturity of human umbilical cord blood T lymphocytes. *Proc Natl Acad Sci U S A* 1992;**89**:10006–10.
6. Ruggeri L, Capanni M, Casucci M, Volpi I, Tosti A, Perruccio K, Urbani E, Negrin RS, Martelli MF, Velardi A. Role of natural killer cell alloreactivity in HLA-mismatched hematopoietic stem cell transplantation. *Blood* 1999;**94**:333–9.
7. Ruggeri L, Capanni M, Urbani E, *et al.* Effectiveness of donor natural killer cell alloreactivity in mismatched hematopoietic transplants. *Science* 2002;**295**:2097–100.
8. Cooley S, McCullar V, Wangen R, Bergemann TL, Spellman S, Weisdorf DJ, Miller JS. KIR reconstitution is altered by T cells in the graft and correlates with clinical outcomes after unrelated donor transplantation. *Blood* 2005;**106**:4370–6.
9. Komanduri KV, St John LS, de Lima M, *et al.* Delayed immune reconstitution after cord blood transplantation is characterized by impaired thymopoiesis and late memory T cell skewing. *Blood* 2007;**110**:4543–51.
10. Giraud P, Thuret I, Reviron D, Chambost H, Brunet C, Novakovitch G, Farnarier C, Michel G. Immune reconstitution and outcome after unrelated cord blood transplantation: a single paediatric institution experience. *Bone Marrow Transplant* 2000;**25**:53–7.
11. Locatelli F, Maccario R, Comoli P, *et al.* Hematopoietic and immune recovery after transplantation of cord blood progenitor cells in children. *Bone Marrow Transplant* 1996;**18**:1095–101.
12. Gaddy J, Risdon G, Broxmeyer HE. Cord blood natural killer cells are functionally and phenotypically immature but readily respond to interleukin-2 and interleukin-12. *J Interferon Cytokine Res* 1995;**15**:527–36.
13. Bradstock KF, Luxford C, Grimsley PG. Functional and phenotypic assessment of neonatal human leucocytes expressing natural killer cell-associated antigens. *Immunol Cell Biol* 1993;**71**:535–42.
14. Phillips JH, Hori T, Nagler A, Bhat N, Spits H, Lanier LL. Ontogeny of human natural killer (NK) cells: fetal NK cells mediate cytolytic function and express cytoplasmic CD3 epsilon,delta proteins. *J Exp Med* 1992;**175**:1055–66.
15. Gaddy J, Broxmeyer HE. Cord blood CD16⁺ 56⁻ cells with low lytic activity are possible precursors of mature natural killer cells. *Cell Immunol* 1997;**180**:132–42.
16. Igarashi T, Wynberg J, Srinivasan R, Becknell B, McCoy JP Jr, Takahashi Y, Suffredini DA, Linehan WM, Caligiuri MA, Childs RW. Enhanced cytotoxicity of allogeneic NK cells with killer immunoglobulin-like receptor ligand incompatibility against melanoma and renal cell carcinoma cells. *Blood* 2004;**104**:170–7.
17. Imai C, Iwamoto S, Campana D. Genetic modification of primary natural killer cells overcomes inhibitory signals and induces specific killing of leukemic cells. *Blood* 2005;**106**:376–83.
18. Kondo E, Topp MS, Kiem HP, Obata Y, Morishima Y, Kuzushima K, Tanimoto M, Harada M, Takahashi T, Akatsuka Y. Efficient generation of antigen-specific cytotoxic T cells using retrovirally transduced CD40-activated B cells. *J Immunol* 2002;**169**:2164–71.
19. Nakao S, Takami A, Takamatsu H, *et al.* Isolation of a T-cell clone showing HLA-DRB1*0405-restricted

- cytotoxicity for hematopoietic cells in a patient with aplastic anemia. *Blood* 1997;**89**:3691–9.
20. Ogawa H, Tamaki H, Ikegame K, *et al.* The usefulness of monitoring WT1 gene transcripts for the prediction and management of relapse following allogeneic stem cell transplantation in acute type leukemia. *Blood* 2003;**101**:1698–704.
 21. McKenzie RS, Simms PE, Helfrich BA, Fisher RI, Ellis TM. Identification of a novel CD56⁻ lymphokine-activated killer cell precursor in cancer patients receiving recombinant interleukin 2. *Cancer Res* 1992;**52**:6318–22.
 22. Mavilio D, Lombardo G, Benjamin J, *et al.* Characterization of CD56⁻/CD16⁺ natural killer (NK) cells: a highly dysfunctional NK subset expanded in HIV-infected viremic individuals. *Proc Natl Acad Sci U S A* 2005;**102**:2886–91.
 23. Jacobs R, Stoll M, Stratmann G, Leo R, Link H, Schmidt RE. CD16⁻ CD56⁺ natural killer cells after bone marrow transplantation. *Blood* 1992;**79**:3239–44.
 24. Ayello J, van de Ven C, Fortino W, *et al.* Characterization of cord blood natural killer and lymphokine activated killer lymphocytes following ex vivo cellular engineering. *Biol Blood Marrow Transplant* 2006;**12**:608–22.
 25. Moretta A, Maccario R, Fagioli F, *et al.* Analysis of immune reconstitution in children undergoing cord blood transplantation. *Exp Hematol* 2001;**29**:371–9.
 26. Salih HR, Antropius H, Gieseke F, Lutz SZ, Kanz L, Rammensee HG, Steinle A. Functional expression and release of ligands for the activating immunoreceptor NKG2D in leukemia. *Blood* 2003;**102**:1389–96.
 27. Costello RT, Sivori S, Marcenaro E, Lafage-Pochitaloff M, Mozziconacci MJ, Revirion D, Gastaut JA, Pende D, Olive D, Moretta A. Defective expression and function of natural killer cell-triggering receptors in patients with acute myeloid leukemia. *Blood* 2002;**99**:3661–7.
 28. Fauriat C, Just-Landi S, Mallet F, Arnoulet C, Sainty D, Olive D, Costello RT. Deficient expression of NCR in NK cells from acute myeloid leukemia: evolution during leukemia treatment and impact of leukemia cells in NCRdull phenotype induction. *Blood* 2007;**109**:323–30.

The DNA demethylating agent 5-aza-2'-deoxycytidine activates NY-ESO-1 antigenicity in orthotopic human glioma

Atsushi Natsume^{1*}, Toshihiko Wakabayashi^{1,2}, Kunio Tsujimura^{3*}, Shinji Shimato¹, Motokazu Ito¹, Kiyotaka Kuzushima³, Yutaka Kondo⁴, Yoshitaka Sekido⁴, Hitomi Kawatsura¹, Yuji Narita⁵ and Jun Yoshida^{1,2}

¹Department of Neurosurgery, Nagoya University School of Medicine, Nagoya, Japan

²Center for Genetic and Regenerative Medicine, Nagoya University Hospital, Nagoya, Japan

³Division of Immunology, Aichi Cancer Center Research Institute, Nagoya, Japan

⁴Division of Molecular Oncology, Aichi Cancer Center Research Institute, Nagoya, Japan

⁵Department of Tissue Engineering, Nagoya University School of Medicine, Nagoya, Japan

Cancer/testis antigens (CTAs) are considered to be suitable targets for the immunotherapy of human malignancies. It has been demonstrated that in a variety of tumors, the expression of certain CTAs is activated *via* the demethylation of their promoter CpG islands. In our study, we have shown that while the composite expression of 13 CTAs in 30 human glioma specimens and newly established cell lines from the Japanese population was nearly imperceptible, the DNA-demethylating agent 5-aza-2'-deoxycytidine (5-aza-CdR) markedly reactivated CTA expression in glioma cells but not in normal human cells. We quantified the diminished methylation status of NY-ESO-1-one of the most immunogenic CTAs-following 5-aza-CdR treatment by using a novel PyrosequencingTM technology and methylation-specific PCR. Microarray analysis revealed that 5-aza-CdR is capable of signaling the immune system, particularly, human leukocyte antigen (HLA) class I upregulation. ⁵¹Cr-release cytotoxicity assays and cold target inhibition assays using NY-ESO-1-specific cytotoxic T lymphocyte (CTL) lines demonstrated the presentation of *de novo* NY-ESO-1 antigenic peptides on the cell surfaces. In an orthotopic xenograft model, the systemic administration of 5-aza-CdR resulted in a significant volume reduction of the transplanted tumors and prolonged the survival of the animals after the adoptive transfer of NY-ESO-1-specific CTLs. These results suggested that 5-aza-CdR induces the expression of epigenetically silenced CTAs in poorly immunogenic gliomas and thereby presents a new strategy for tumor immunotherapy targeting 5-aza-CdR-induced CTAs.

© 2008 Wiley-Liss, Inc.

Key words: glioma; cancer-testis antigens; DNA methylation; immunotherapy; NY-ESO-1

Over the last decade, there has been major progress in the identification and characterization of human tumor antigens recognized by the host immune system. A subgroup of tumor antigens, commonly referred to as cancer/testis antigens (CTAs), are expressed only in the tissues of the testis, ovary and placenta under normal conditions, but are also expressed in various types of human tumors.^{1,2} Since normal CTA-expressing tissues do not express major histocompatibility complex (MHC) class I molecules, CD8 T cells cannot recognize CTAs expressed on these tissues, suggesting that CTAs are the ideal targets for tumor immunotherapy. CTAs and genes were originally identified through a variety of methods. These include T-cell epitope labeling,³ serological analysis of cDNA expression libraries (SEREX),^{4,5} differential gene expression analysis⁶ and bioinformatics methods.^{7–9} In particular, NY-ESO-1 is the most immunogenic CTA discovered thus far, and it is considered to be a highly promising therapeutic target for immunotherapy.¹⁰ To date, very little is known regarding the physiological function(s) of these antigens or the mode in which the expression of their gene families is regulated.

Epigenetic alterations, including hypermethylation of promoter CpG islands, histone deacetylation of tumor suppressor and tumor-related genes,^{11–13} and global DNA hypomethylation,^{14,15} have been recognized as important contributors to carcinogenesis in humans. Global DNA hypomethylation has been observed in various neoplasms and is considered to occur at the early stages of

tumor development.^{16–18} However, it has been shown that the expression of certain CTA genes is reactivated in cancerous cells; this could be due to a loss of epigenetic regulation as observed when methylated chromatin regions are demethylated or when deacetylated histones are acetylated.¹⁹ Therefore, recent evidence shows that the deregulation of the DNA methylation apparatus that occurs during cancer development could provide new therapeutic targets for cancer treatment.

The DNA demethylating agent 5-aza-2'-deoxycytidine (5-aza-CdR, decitabine) is a cytosine analogue that is incorporated into DNA during replication. It covalently binds DNA methyltransferase and inhibits its activity, leading to genome-wide demethylation.^{20–24} There have been several studies demonstrating the ability of 5-aza-CdR to activate the gene expression of CTAs *in vitro* and *in vivo*, which may be silenced by the hypermethylation of their promoters. This drug has been used in clinical studies for the treatment of chronic myelogenous leukaemia (CML), sickle cell anaemia and myelodysplastic syndrome (MDS).^{20,25–27} Previous evidence has clearly defined the epigenetic regulatory role of DNA methylation in the constitutive expression of CTAs by cutaneous melanoma cells and renal cancer cells and has demonstrated that *in vitro* treatment with 5-aza-CdR upregulated their expression in neoplastic cells.^{28,29}

Gliomas are the most common primary tumors of the central nervous system; they account for 30% of adult primary brain tumors. Brain tumors remain difficult to cure despite recent advances in surgical, radiotherapeutic and chemotherapeutic approaches. In particular, there is currently no optimal treatment for glioblastoma multiforme, the most common malignant brain tumor in adults, and patients typically survive for a period less than a year. The poor outcome partly relates to the inability in delivering chemotherapeutic agents through the blood–brain barrier (BBB) and the low effect of radiation on the tumor. Therefore, new and more effective strategies are urgently required. Of these, the establishment of immunotherapy specifically targeting malignant cells is expected to improve tumor prognosis. It has recently been demonstrated that malignant glioma cells express certain known tumor-associated antigens such as HER-2, gp100, MAGE-

This article contains supplementary material available via the Internet at <http://www.interscience.wiley.com/jpages/0020-7136/suppmat>.

Grant sponsor: Grant-in-Aid for Scientific Research (B) from the Ministry of Health, Labor, and Welfare; Grant number: 18390395; Grant sponsor: the Japan Society for the Promotion of Science, Tokyo; Grant sponsor: the Third Team Comprehensive Control Research for Cancer from the Ministry of Health, Labor, and Welfare, Japan; Grant number: 26.

Kunio Tsujimura's current address is: Department of Infectious Diseases, Hamamatsu University School of Medicine, 1-20-1 Handa-yama, Higashi-ku, Hamamatsu 431-3192, Japan.

*Correspondence to: Department of Neurosurgery, Nagoya University School of Medicine, 65 Tsurumai-cho, Showa-ku, Nagoya 466-8550, Japan. E-mail: anatsume@med.nagoya-u.ac.jp or ktsujimu@hama-med.ac.jp

Received 5 July 2007; Accepted after revision 4 December 2007

DOI 10.1002/ijc.23407

Published online 31 January 2008 in Wiley InterScience (www.interscience.wiley.com).

1 and IL-13 receptor $\alpha 2$.³⁰⁻³⁷ However, CTA profiling of glioma cells, in particular, in the Asian population remains unknown.

In our study, we analyzed the expression of 13 CTA genes (*MAGE-1*, *MAGE-3*, *MAGE-4*, *MAGE-6*, *MAGE-10*, *MAGE-3/6*, *LAGE-1*, *CT7*, *SCP-1*, *SSX-1*, *SSX-2*, *SSX-4* and *NY-ESO-1*) in 30 glioma tissues, 5 human glioma cell lines and 3 newly established cell lines from the Japanese population. Subsequently, the role of 5-aza-CdR in the regulation of the expression of various CTAs in glioma cells was analyzed. Finally, we demonstrated that NY-ESO-1, one of the most antigenic CTAs, is effectively induced in human glioma cells by 5-aza-CdR, and that these glioma cells forcibly expressing NY-ESO-1 show *in vitro* and *in vivo* sensitivity to NY-ESO-1-specific cytotoxic T lymphocytes (CTLs). Our present study provides the basis to establish novel immunotherapeutic approaches in glioma patients.

Material and methods

Cells

The human glioma cell lines U251 (human leukocyte antigen (HLA)-A2), SKMG1 (HLA-A24), AO2 (HLA-A3), U87MG (HLA-A2) and T98 (HLA-A2) were obtained from the Memorial Sloan-Kettering Cancer Institute (New York, NY) and maintained in Eagle's minimal essential medium (MEM) at 37°C in a humidified atmosphere of 5% CO₂ in air. A human osteosarcoma cell line, namely, SaOS-2 (NY-ESO-1+, HLA-A2), was kindly provided by Dr. Y. Nishida (Department of Orthopaedics, Nagoya University, Nagoya, Japan) and maintained in Dulbecco's modified Eagle's medium (DMEM; Nissui, Tokyo, Japan). A human myeloid leukaemia cell line K562 and the HLA-A*0201-transfected T2 cell line (T2.A2) were maintained in RPMI 1640 (Invitrogen, Carlsbad, CA). The medium was supplemented with 10% fetal bovine serum (FBS), 5 mM L-glutamine, 2 mM nonessential amino acids, and antibiotics (100 U/ml penicillin and 100 µg/ml streptomycin). Commercially available normal human astrocytes (NHA; Cambrex, Baltimore, MD) maintained in AGM medium with BulletKit supplement (Cambrex), human aortic smooth muscle cells (AoSMC; Cambrex), human adult fibroblasts (NHDF-ad; Cambrex) maintained in DMEM with 10% FBS, and human epidermal keratinocytes (NHEK, Kurabo, Osaka, Japan) maintained in Epilife medium (Cascade Biologics, Nottinghamshire, UK) supplemented with HuMedia-KG (Kurabo) were used as normal cells.

Reagents and peptides

A vial containing 5 mg lyophilized powder of 5-aza-CdR was obtained (Sigma-Aldrich, St. Louis, MO). The vial was reconstituted with 20 ml sterile water to obtain a 1 mM solution, and it was stocked at 4°C. The HLA-A2-binding NY-ESO-1 peptide, p157-165 (SLLMWITQC), which was initially identified using the T-cell line NW38-IVS-1³⁸ and the HLA-A2-binding IL-13R $\alpha 2$ peptide, p345-354 (WLPFGFILI), which was identified previously,³⁷ was synthesized by Thermo Electron GmbH (>90% purity) (Ulm, Germany), and solubilized in 50% dimethyl sulphoxide (DMSO)/water.

Collection of surgical specimens

Thirty tumor samples were collected at the Nagoya University School of Medicine from patients whose tumors were histologically diagnosed as gliomas (WHO Grade II, III and IV). Genetic analysis in our study was approved by the ethical committee of Nagoya University Hospital. All patients provided written informed consent. All tissues were frozen immediately and stored at -80°C until use.

Primary-culture cells derived from patients with high-grade gliomas

Tumor tissues were derived from 3 patients with high-grade gliomas who had undergone surgical resection in Nagoya University Hospital, Nagoya, Japan; the tissues were primary-cultured as

follows. Immediately after the brain tumors were removed from the patients, the tissues were homogenized and digested with 1% DNase and 0.1% trypsin for 30 min at 37°C and centrifuged at 800 rpm for 5 min. The cells were seeded at a density of 2×10^6 cells per 100-mm dish and maintained in DMEM supplemented with 10% FBS, 5 mM L-glutamine, 2 mM nonessential amino acids, and antibiotics (100 U/ml penicillin and 100 µg/ml streptomycin). The cells were then incubated in a standard tissue culture incubator (100% relative humidity and 5% CO₂). After achieving 80–90% confluence, they were subcultured onto a new 100-mm plate at a density of 2×10^6 . The established cell lines were designated as NNS-10, NNS-11 and NNS-12. All cells were immunocytochemically confirmed as glioma cells based on their expression of glial-fibrillary acidic protein (GFAP).

In vitro treatment of cultured cells with 5-aza-CdR

Treatment with 5-aza-CdR was performed as described in a previous study.²⁹ Cells were seeded at a density of 1.0×10^5 cells/well in a 6-well plate, and placed at 37°C overnight in a 5% CO₂ incubator. The next day, the cell culture medium was replaced with fresh medium containing 0.1, 1 and 10 µM 5-aza-CdR. The medium was changed every 12 hr for 2 days. The plates were wrapped in aluminum foil to avoid light exposure. At the end of the treatment, the medium was replaced with fresh medium without 5-aza-CdR, and the cells were cultured for an additional 48 hr.

RNA extraction

RNA was isolated from 25 to 50 mg of tissue/sample by using Trizol (Invitrogen) according to the manufacturer's protocol. RNA was finally resuspended in nuclease-free water.

Conventional reverse transcription PCR

cDNA was synthesized from 1 µg total RNA by using random hexamers and the Superscript II reverse transcription (RT) kit (Invitrogen), according to the manufacturer's protocol. For each PCR, 2 µl cDNA was used in a 20-µl reaction volume containing 200 mM dNTPs, 1 mM sense and antisense primers, 1.25 mM MgCl₂, 2 µl 10× PCR buffer, and 0.5 U Taq polymerase (Applied Biosystems, Foster City, CA). The PCR primers used were those listed in the Ref. 39 β-actin was used as the endogenous control. The cycling parameters were as follows: denaturation at 95°C for 45 s, primer annealing at 55°C for 45 s, and 35 cycles of extension at 72°C for 60 s. PCR cycling was preceded by an initial denaturation at 95°C for 5 min, followed by final extension at 72°C for 5 min. The PCR products were analyzed by electrophoresis on a 1.5% agarose gel; this was followed by staining with ethidium bromide. If no signal was observed, the remaining PCR products were amplified by an additional 15 cycles and analyzed again to confirm the absence of the signal.

Quantitative RT-PCR for NY-ESO-1 expression

After synthesis of the first cDNA strand as described earlier, quantitative RT-PCR was performed on the LightCycler real-time RT-PCR system (version 3.39) (Roche, Mannheim, Germany), using the FastStart Taqman Probe Master (ROX) (Roche) along with sets of primers and Universal ProbeLibrary probes (Roche) designed online with ProbeFinder version 2.40 (Roche). Probes specific for NY-ESO-1 were as follows: forward primer: 5'-TGTCGGCAACATACTGACT-3', reverse primer: 5'-ACT-GCGTGATCCACATCAAC-3', and Universal ProbeLibrary probe Human No. 67 (Roche), which yields a 111-nt amplicon. The endogenous reference gene *GAPDH* was amplified by the forward primer: 5'-AGCCACATCGCTCAGACAC-3', reverse primer: 5'-CGCCCAATACGACCAAATC-3', and Universal ProbeLibrary probe Human No. 60, which yields a 67-nt amplicon. Each sample was amplified as follows: 1 cycle at 95°C for 10 min followed by 40 cycles at 95°C for 15 s and 60°C for 1 min. cDNA from SaOS-2 was used to generate the standard curves for NY-

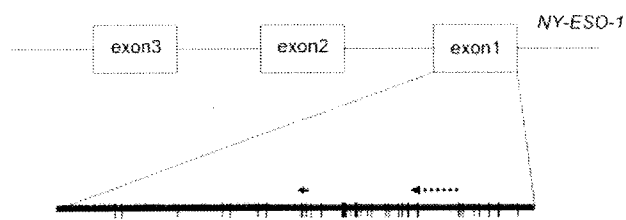


FIGURE 1 – Schematic view of the *NY-ESO-1* gene region analyzed in this study. Vertical lines indicate CpG dinucleotides, the solid arrow indicates the Pyrosequencing primer, and the broken arrows indicate the location of MSP primers.

ESO-1 and *GAPDH*. Standardization of samples was achieved by dividing the copy number of the target gene *NY-ESO-1* by that of the *GAPDH* gene. Values were expressed as ratios relative to *NY-ESO-1* expression in SaOS-2.

Western blot analysis

Cells treated with 5-aza-CdR (1 μ M) and untreated cells were lysed in a buffer containing protease inhibitors. Protein samples (45 μ g) were denatured at 100°C for 5 min and subsequently applied to each well and electrophoresed on a 12.5% polyacrylamide gel. After transferring the proteins to a polyvinylidene difluoride (PVDF) membrane, it was blocked with 3% low-fat skim milk, incubated with a monoclonal antibody (mAb) against *NY-ESO-1* (ES121; Zymed, San Francisco, CA), and then washed and incubated with an horseradish peroxidase (HRP)-labelled secondary Ab. Visualization was performed using an enhanced chemiluminescence technique.

NY-ESO-1 promoter DNA methylation analyses

Methylation-specific PCR (MSP)⁴⁰ and PyrosequencingTM technology⁴¹ were used to determine the methylation status of the CpG island region of *NY-ESO-1*. None of the sequences identified in the *NY-ESO-1* promoter region fulfilled the criteria for CpG islands (length, >200 bp, G + C content, >50%, observed CpG/expected CpG ratio, ≥ 0.6).⁴² The CpG islands and the location of the primers in exon 1 for DNA methylation analyses are shown in Figure 1. Genomic DNA isolation and sodium bisulphite conversion were performed as described previously.⁴³ The primer sequences and annealing temperatures of MSP were as reported previously.⁴⁴ The primer sequences for PyrosequencingTM were designed using PSQ Assay Design (Biotage, Uppsala, Sweden). A 50- μ l PCR was carried out in 60 mM Tris \pm HCl (pH 8.5), 15 mM ammonium sulphate, 2 mM MgCl₂, 10% DMSO, 1 mM dNTP mix, 1 U Taq polymerase, 5 pmol forward primer (5'-GGGTTGAATGGATGTTGTAG-3'), 50 pmol reverse primer (5'-CRCCACCAAACTATCAA-3'), 50 pmol biotinylated universal primer (5'-GGGACACCGCTGATCGTTTACRCCACCAAACTATCAA-3') and ~50 ng bisulphite-treated genomic DNA. The forward primer contains a 20-bp linker sequence on the 5' end that is recognized by biotin-labeled primers; thus, the final PCR product can be purified using Sepharose beads. PCR cycling conditions were as follows: 95°C for 30 s, 60°C for 45 s and 72°C for 45 s for 55 cycles. The biotinylated PCR product was purified and made single-stranded to act as a template in a pyrosequencing reaction using the Pyrosequencing Vacuum Prep Tool (Pyrosequencing, Westborough, MA), as recommended by the manufacturer. In brief, the PCR product was bound to Streptavidin Sepharose HP (Amersham Biosciences, Uppsala, Sweden), and the Sepharose beads containing the immobilized PCR product were purified, washed, denatured using 0.2 M NaOH solution and washed again. Then, 0.3 mM pyrosequencing primer (5'-TGAATGGATGTTGTAGATG-3') was annealed to the purified single-stranded PCR product, and pyrosequencing was performed using the PSQ HS

96Pyrosequencing System (Pyrosequencing). Methylation quantification was performed using the provided software.

Flow cytometric analysis

Glioma cells were treated with 5-aza-CdR as described earlier. The treated and untreated cells were stained with anti-HLA class-I mAbs (W6/32; kindly provided by Dr. K. Itoh, Kurume University, Kurume, Japan) or isotype control mouse IgG2a followed by staining with fluorescein isothiocyanate (FITC)-labelled anti-mouse IgG Abs. Flow cytometric analysis of stained cells was performed by using FACS Calibur (Becton Dickinson, San Jose, CA).

Induction of HLA-A2-restricted *NY-ESO-1*-specific CTL lines by peptide-pulsed dendritic cells

Peripheral blood mononuclear cells (PBMCs) from healthy volunteers genetically typed as HLA-A2-positive by SRL, (Tokyo, Japan) were isolated using Ficoll-Paque (Amersham Biosciences). Peptide-pulsed dendritic cells (DCs) were prepared from donor-derived PBMCs, as described previously³⁷ with minor modifications. In brief, the plastic adherent cells from PBMCs were cultured in AIM-V medium (Life Technologies, Gaithersburg, MD) supplemented with recombinant human granulocyte/macrophage-colony stimulating factor (rhGM-CSF, 500 U/ml) and rhIL-4 (500 U/ml) at 37°C in a humidified CO₂ (5%) incubator. After 6 days, the culture medium was removed, and the immature DCs were cultured in AIM-V supplemented with rhGM-CSF (500 U/ml), recombinant human interleukin (rhIL)-4 (500 U/ml), rhIL-6 (1,000 U/ml), recombinant human tumor necrosis factor- α (10 ng/ml), and IL-1 β (10 ng/ml). All cytokines used were purchased from Strathmann Biotech AG, Hanover, Germany. Mature DCs were harvested after another 2 days, resuspended in AIM-V medium at 1 \times 10⁶ cells/ml with the peptide (10 μ g/ml), and incubated for 4 hr at 37°C. The peptide-pulsed DCs were then treated with mitomycin-C, washed, and finally resuspended in AIM-V medium supplemented with 10% human AB serum. Autologous CD8⁺ T cells were enriched from PBMCs by using magnetic microbeads (Miltenyi Biotec, Auburn, CA) and were added (1 \times 10⁶/well) to the peptide-pulsed DCs (1 \times 10⁵/well) in 2 ml AIM-V medium supplemented with 10% human AB serum, 1,000 U/ml rhIL-6, and 10 ng/ml rhIL-12 in each well of 24-well tissue culture plates. On day 7, the lymphocytes were restimulated with mitomycin-C-treated autologous DCs pulsed with peptides in AIM-V medium supplemented with 10% human AB serum, rhIL-2 and rhIL-7 (10 U/ml each). One week later and on a weekly basis thereafter, the responder cells were restimulated with peptide-pulsed DCs in a medium supplemented with rhIL-2 and rhIL-7 (10 U/ml each). The induction of *NY-ESO-1*-specific CTL lines was attempted 3 times.

CTL assay

The susceptibility of the untreated and 5-aza-CdR-treated U251 glioma cells (HLA-A2) to HLA-A2-restricted *NY-ESO-1*-specific CTL lines was evaluated by a standard 4-h ⁵¹Cr-releasing assay at various (effector:target) E:T ratios. The percentage specific lysis was calculated as follows: 100 \times (experimental release – spontaneous release)/(maximum release – spontaneous release).

Cold target inhibition assay

The cold target inhibition assay was performed as described previously.⁴⁵ In brief, T2.A2 cells were incubated with the *NY-ESO-1* peptide or the irrelevant IL-13R α 2 peptide at a concentration of 10 μ M for 1 hr. After extensive washing, the indicated numbers of peptide-loaded cells were incubated with 2 \times 10⁴ cytotoxic effector cells for 1 hr, and then 2 \times 10³ ⁵¹Cr-labeled, 5-aza-CdR-treated U251 glioma cells were added to each well. Cytotoxicity was assessed at the E:T ratio of 10:1 as described earlier.

TABLE 1 - RT-PCR ANALYSIS FOR EXPRESSION OF CANCER-TESTIS ANTIGENS IN GLIOMA TISSUES

Patient	Pathology	NY-ESO-1	MAGE-1	MAGE-3	MAGE-4	MAGE-6	MAGE-10	MAGE-3/6	LAGE-1	CT7	SCP-1	SSY-1	SSX-2	SSX-4
1	GBM		■											
2	GBM													
3	GBM													
4	GBM													
5	GBM							■						
65	GBM													
194	GBM													
195	GBM													
197	GBM													
198	GBM													
199	GBM													
6	AA													
7	AA													
8	AA													
9	AA													
12	AA	■	■				■	■						
14	AA				■									
67	AA													
69	AA													
78	AA													
199	AA													
199	AA													
202	AA													
203	AA													
18	AS													
17	AS													
18	AS													
192	AS													
193	AS													
200	AS													
Rate		(1/30)	(2/30)	(0/30)	(1/30)	(0/30)	(1/30)	(2/30)	(0/30)	(0/30)	(0/30)	(0/30)	(0/30)	(0/30)

We investigated the composite expression of 13 CTAs in 30 human glioma specimens by RT-PCR analysis. MAGE-4, MAGE-10 and NY-ESO-1 were expressed in only 1 sample out of 30, and MAGE-1 and MAGE3/6 were expressed in 2 samples. Other CTAs were all negative in the 30 brain tumor specimens tested. The expression pattern of these did not correlate with the histological grades of gliomas.

Black and white boxes indicate positive and negative expression, respectively.

GBM, glioblastoma multiforme (WHO Grade IV); AA, anaplastic astrocytoma (Grade III); AS, astrocytoma (Grade II).

Orthotopic glioma xenograft model

Female nonobese diabetic/severe combined immunodeficiency disease (NOD/SCID) mice aged 5 weeks were used in the experiments. All mice were purchased from SLC, Hamamatsu, Japan. They were maintained under specific pathogen-free conditions in the animal facility of Nagoya University School of Medicine. Animal experiments were performed according to the principles enunciated in the Guide for the Care and Use of Laboratory Animals prepared by the Office of the Prime Minister of Japan.

Mice were anaesthetized with an intraperitoneal injection of pentobarbital (60–70 mg/kg body weight). After shaving the hair and incising the scalp, a burr hole was made in the skull 3 mm lateral to the midline and 4 mm posterior to the bregma using a dental drill. The head of each mouse was fixed in a stereotactic apparatus with ear bars, and 2×10^5 U251 cells in 2 μ l PBS were stereotactically injected over 4 min at a depth of 2 mm below the dura mater. A sterile Hamilton syringe fitted with a 26-gauge needle was used with a microsyringe pump. The needle was retained in the brain for an additional 2-min duration and then slowly withdrawn.

To test the induction of NY-ESO-1 in orthotopic glioma xenografts, 5-aza-CdR [0.2 mg/kg, intraperitoneally (i.p)] was administered every 12 hr for 4 consecutive days (8 pulses) starting on day 14 after glioma inoculation. The control brain tumor model was treated under similar experimental conditions by an i.p. PBS injection.

To determine whether the treated cells upregulated the NY-ESO-1 expression, the mice were killed on day 3 after the final 5-aza-CdR injection. The brain tumors were removed for RT-PCR for NY-ESO-1.

Tumor-inoculated NOD/SCID mice were randomly divided into 4 treatment groups (10 animals each) to examine the treatment efficacy of NY-ESO-1-specific CTLs in combination with 5-aza-CdR. The animals in the various groups were then injected as follows: Group I, PBS (i.p., 8 pulses starting from the day after tumor inoculation) and PBS (2 μ l) intratumorally (i.t.) 6 days after tumor inoculation; Group II, PBS i.p. (8 pulses) and bulk CTLs (i.t., 1×10^6 cells/mouse in 2 μ l); Group III, 5-aza-CdR i.p. (0.2 mg/kg, 8 pulses) and PBS (i.t., 2 μ l); Group IV, 5-aza-CdR i.p. (0.2 mg/kg, 8 pulses) and bulk CTLs (i.t., 1×10^6 cells/mouse in 2 μ l). Five mice in each group were euthanized using CO₂ inhalation on day 21 after tumor injection. The mice were transcardially perfused with 4% paraformaldehyde. The brain tissue was postfixed overnight, embedded in paraffin, and then cut into 5- μ m serial horizontal sections. Tissue sections were stained by the standard haematoxylin and eosin technique. The growth inhibitory effect was evaluated by measuring the long (*a*) and short (*b*) axes in the coronal section showing the maximal area of each tumor. The approximate volume of the tumor (*V*) was calculated according to the formula, V (mm³) = $a \times b^2/2$. In addition, the survival times of all the remaining mice were recorded.

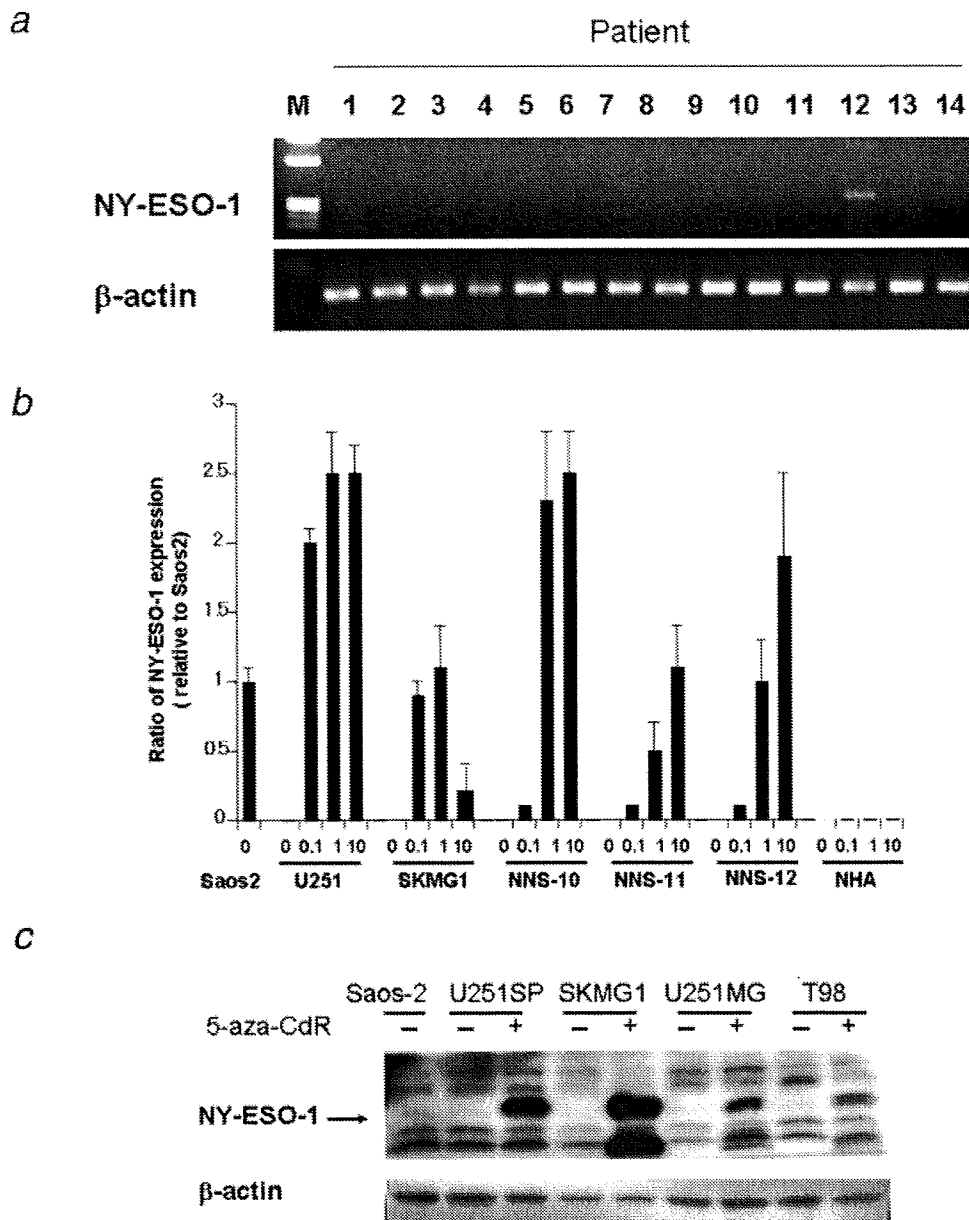


FIGURE 2 – *NY-ESO-1* expression in human gliomas. (a) RT-PCR for *NY-ESO-1* in surgical specimens of gliomas. The summarized data is presented in Table I. (b) Real-time quantitative RT-PCR showing *NY-ESO-1* induction in glioma cells but not in normal cells by 5-aza-CdR. The expression of *NY-ESO-1* was upregulated in U251, SKMG1, and primary-cultured glioma cells (NNS-10, NNS-11 and NNS-12) treated with 0.1, 1 and 10 μ M 5-aza-CdR but not in normal astrocytes (NHA). 5-aza-CdR (10 μ M) induced toxicity in SK-MG-1, leading to decreased *NY-ESO-1* expression. (c) Detection of *NY-ESO-1* in glioma cell lines by western blot analysis. We prepared cell lysates of the untreated (–) gliomas (U251 (sublines SP and MG), SKMG1 and T98) and those treated (+) with 5-aza-CdR (1 μ M) and *NY-ESO-1*-positive osteosarcomas (SaOs-2, as a positive control); western blotting analysis was conducted using an anti-*NY-ESO-1* mAb.

The statistical significance of the difference in tumor volumes and Kaplan–Meier survival curves was determined by analysis of variance (ANOVA) (StatView, SAS Institute, Cary, NC) with Bonferroni's correction for multiple comparisons and the log-rank test (StatView), respectively.

Results

Expression of individual CTA genes in human gliomas and glioma cell lines

Although the expression frequencies of many CTAs in a variety of neoplasms have been determined, their expression in human gliomas remains unclear, and the expression frequency of CTAs varies

drastically among ethnic groups.³⁹ It would be useful to analyze the expression pattern of CTAs in gliomas in the Japanese population. In our study, RT followed by 35 cycles of amplification revealed that the expression of CTA genes was nearly imperceptible in human gliomas, and the expression pattern of these genes did not correlate with the histological grades of the gliomas (Table I). *MAGE-4*, *MAGE-10* and *NY-ESO-1* were expressed in only 1 of 30 samples, and *MAGE-1* and *MAGE-3/6* were expressed in 2 samples. The samples were negative for *MAGE-3*, *MAGE-6*, *LAGE-1*, *CT7*, *SCP-1*, *SSX-1*, *SSX-2* and *SSX-4* even after 50 amplification cycles of the 30 brain tumor specimens tested (Fig. 2a and Table I). Moreover, the human glioma cell lines and primary-cultured glioma cells did not test positive for any of the 13 CTAs even after 50 amplifica-

TABLE II - INDUCTION OF CTA EXPRESSION BY 5-AZA-CDR IN GLIOMA CELLS AND NORMAL CELLS

Cell	5-aza-CdR (μ M)	NY-ESO-1	MAGE-1	MAGE-3	MAGE-4	MAGE-6	MAGE-10	MAGE-3/6	LAGE-1	CT7	SCP-1	SSX-1	SSX-2	SSX-4
U251 (glioma)	None													
	0.1	■		■					■					
	1	■		■					■					
	10	■		■					■					
SK-MG-1 (glioma)	None													
	0.1	■							■					
	1	■							■					
	10	■							■					
A02 (glioma)	None													
	0.1			■					■					
	1			■					■					
	10			■					■					■
T98 (glioma)	None													
	0.1	■												
	1	■												
	10	■												
U87MG (glioma)	None													
	0.1										■			■
	1										■			■
	10										■			■
NNS-10 (primary glioma)	None													
	0.1	■		■										
	1	■		■										
	10	■		■										
NNS-11 (primary glioma)	None													
	0.1	■		■										
	1	■		■										
	10	■		■										
NNS-12 (primary glioma)	None													
	0.1	■												
	1	■												
	10	■												
NHA (astrocyte)	None													
	0.1													
	1													
	10													
NHDY (astroblast)	None													
	0.1													
	1													
	10													
AoSMC (smooth muscle cell)	None													
	0.1													
	1													
	10													
NH3K (keratinocyte)	None													
	0.1													
	1													
	10													

We assessed whether CTAs could be induced by 5-aza-CdR treatment in 5 human glioma cell lines, 3 primary glioma cell lines and 4 human normal cells. The cells were treated with 0.1, 1 and 10 μ M 5-aza-CdR every 12 h for 2 consecutive days (4 pulses). The human glioma cell lines and primary-cultured glioma cells did not test positive for any of the 13 CTAs even after 50 amplification cycles. The only exception was *LAGE-1*; SKMG1 and T98 cells constitutively expressed *LAGE-1*. Exposure to 5-aza-CdR invariably induced the expression of *LAGE-1*, *MAGE-1*, *MAGE-3*, *MAGE-4*, *MAGE-3/6*, *SCP-1*, *SSX-1*, *SSX-2*, *SSX-4* and *NY-ESO-1* in CTA-negative glioma cells. Because of toxicity, *NY-ESO-1* expression in SK-MG-1, and *MAGE-3/6* and *LAGE-1* expression in U87MG are not observed when treated with 10 μ M 5-aza-CdR. In contrast to glioma cells, administration of the agent does not induce CTA expression in human astrocytes, fibroblasts, smooth muscle cells and epidermal keratinocytes.

tion cycles (Table II). The only exception was *LAGE-1*; SKMG1 and T98 cells constitutively expressed *LAGE-1*.

Effect of 5-aza-CdR on glioma cells and normal human cells in vitro

We assessed whether CTAs could be induced by 5-aza-CdR treatment in 5 human glioma cell lines and 3 primary glioma cell lines. The glioma cells were treated with 0.1, 1 and 10 μ M 5-aza-CdR every 12 hr for 2 consecutive days (4 pulses). Table II summarizes the expression of the 13 CTA genes detected by RT-PCR in glioma cell lines treated with 0.1, 1 and 10- μ M 5-aza-CdR. Exposure to 5-aza-CdR invariably induced the expression of *LAGE-1*, *MAGE-1*, *MAGE-3*, *MAGE-4*, *MAGE-3/6*, *SCP-1*, *SSX-1*, *SSX-2*, *SSX-4* and *NY-ESO-1* in CTA-negative glioma cells. Among these, we focused on *NY-ESO-1*-the most immunogenic

CTA. Real-time quantitative RT-PCR was performed to quantitate *NY-ESO-1* expression in U251, SK-MG-1 and the primary-cultured glioma cells derived from patients (NNS-10, NNS-11 and NNS-12). These results were then compared with those of the *NY-ESO-1*-expressing SaOS-2 cells (Fig. 2b). The expression of *NY-ESO-1* was invariably induced by 5-aza-CdR in all glioma cells tested although the efficiency varied among cells; in particular, 10 μ M 5-aza-CdR induced toxicity in SK-MG-1, leading to decreased *NY-ESO-1* expression. Similar toxicity occurred in U87MG cells (Table II).

It is particularly important to ensure that CTA is not induced in normal cells, including normal brain cells, in order to prevent them from being targets of CTA-specific immune responses. We therefore treated human astrocytes, fibroblasts, smooth muscle cells and epidermal keratinocytes with 5-aza-CdR. In contrast to

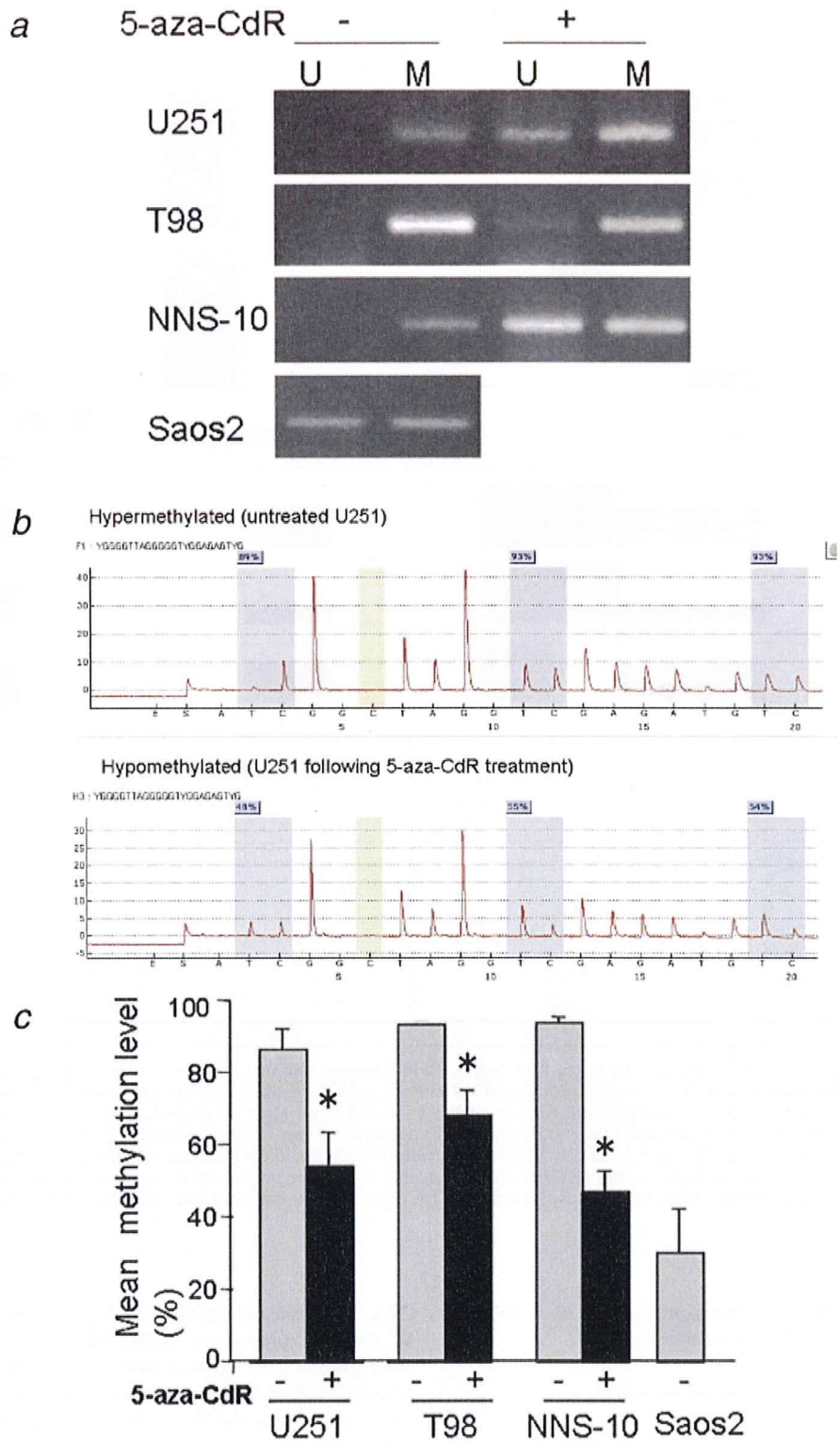


FIGURE 3 – *NY-ESO-1* methylation analyses. (a) DNA methylation of the *NY-ESO-1*-gene was measured by MSP. The *NY-ESO-1* is heavily methylated in glioma cells but not in SaOS2 cells before 5-aza-CdR treatment, and it is hypomethylated following 5-aza-CdR exposure. U and M, reactions for unmethylated and methylated sequences, respectively. (b) Representative pyrograms of hyper- and hypomethylation. The sequence in the upper part of each pyrogram represents the sequence under investigation. The sequence below the pyrogram indicates the sequentially added nucleotides. The gray regions indicate the analyzed C/T sites; the percentage values for the respective cytosine methylation are provided above them. Yellow regions indicate the positions where a cytosine was added to verify the complete conversion from unmethylated cytosine to thymine. (c) Quantitative analyses of *NY-ESO-1* methylation by pyrosequencing. Mean methylation levels \pm SD were 86.3% \pm 5.5%, 93.3% \pm 0.6% and 93.3% \pm 1.5% for U251, T98 and NNS-10 glioma cells, respectively, while it was 30% \pm 12% for SaOS2 cells constitutively expressing *NY-ESO-1*. Following 5-aza-CdR treatment (+), methylation levels were significantly decreased to 54% \pm 9.1%, 68% \pm 6.9% and 46.7% \pm 5.7% for U251, T98 and NNS-10. * $p < 0.05$ compared to untreated (-) cells. [Color figure can be viewed in the online issue, which is available at www.interscience.wiley.com.]

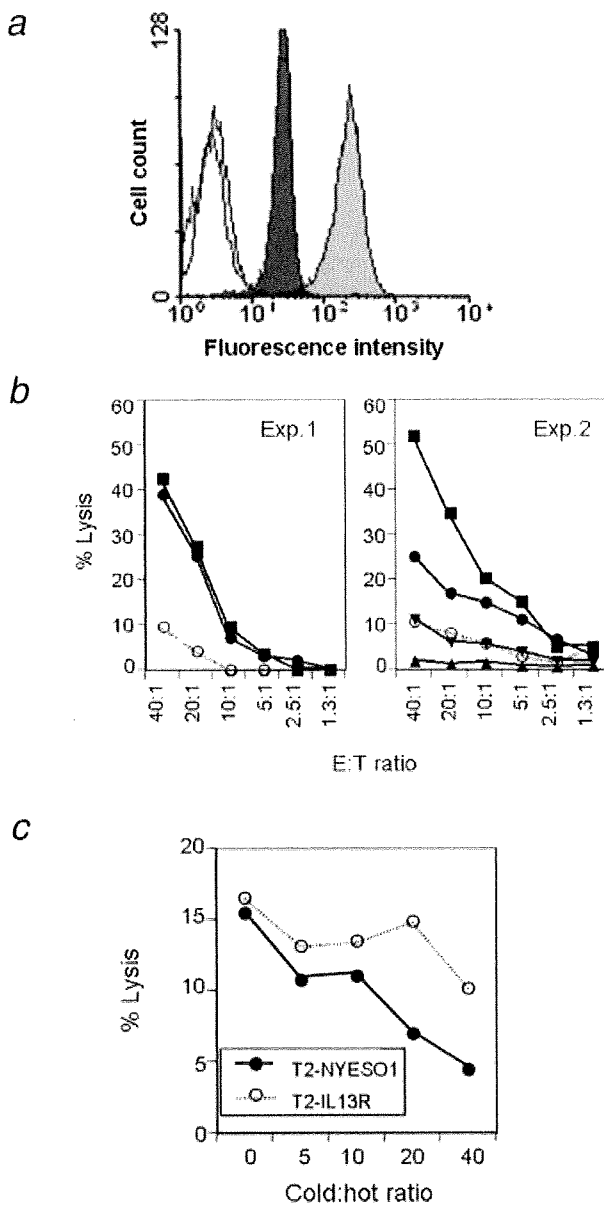


FIGURE 4 – Antigenic potentiation of glioma cells by 5-aza-CdR. (a) Upregulation of HLA class I. Untreated U251 glioma cells (black) and those treated with 5-aza-CdR (gray) were stained with anti-HLA class I mAbs (W6/32). Negative staining of untreated and treated U251 cells with isotype control mouse IgG2a is shown (white). (b) Cytolytic activity of 2 independently induced NY-ESO-1 CTL lines against U251 (HLA-A2⁺) before (○) and after (●) 5-aza-CdR treatment; other NY-ESO-1⁺ glioma cells, SK-MG-1 (A24, ▲); human osteosarcoma cells, SaOS-2 (A2, NY-ESO-1⁺, ■); and human myeloid leukaemia cell line K562 (▼). Exp. 1, Experiment 1; Exp. 2, Experiment 2. (c) The CTL-mediated target cell (5-aza-CdR-treated U251) lysis was blocked using T2.A2 cells that had been loaded with the HLA-A2-binding NY-ESO-1 peptide p157-165 (SLLMWITQC) (●) but not with the control peptide, *i.e.*, the HLA-A2-binding IL-13R α 2 peptide p345-354 (WLPFGFIL) (○). The same CTL line as in the Exp. 2 of Figure 4b was used in the experiment (E:T ratio, 10:1).

glioma cells, administration of the agent did not induce CTA expression in these cells (Fig. 2b and Table II).

To assess whether the induction of CTA mRNA is followed by the production of the appropriate protein, western blotting for NY-ESO-1 was performed using untreated and 5-aza-CdR-treated glioma cell lines. The SaOS-2 osteosarcoma cell line, which constitutively

expresses NY-ESO-1 without 5-aza-CdR treatment, was used as a positive control. As shown in Figure 2c, 23-kDa bands corresponding to NY-ESO-1 were observed in all glioma cell lines treated with 5-aza-CdR but were absent in the untreated cells (all data not shown). This result suggested that the NY-ESO-1 expression was induced after 5-aza-CdR treatment at the protein level as well as the mRNA level.

Quantitative CpG island mapping with PyrosequencingTM

MSP experiments were performed to evaluate the methylation status of NY-ESO-1 in cultured glioma cells. We observed that the NY-ESO-1 is heavily methylated in glioma cells before 5-aza-CdR treatment and becomes hypomethylated following 5-aza-CdR exposure (Fig. 3a). To quantify the methylation of the CpG sites of NY-ESO-1, we employed a novel real-time DNA sequencing technology called PyrosequencingTM. This technology was originally developed for the analysis of single-base variations and enables the precise quantification of incorporated nucleotides at polymorphic positions. Treatment of the DNA with sodium bisulphite converts the epigenetic difference between methylated and unmethylated cytosine into a single-base variation of the C/T type. Therefore, Pyrosequencing is a very suitable tool for methylation analysis. Representative pyrograms for hypermethylated (untreated U251 cells) and hypomethylated (U251 cells following 5-aza-CdR exposure) are shown in Figure 3b. We identified the regions showing the largest differences in methylation and compared methylation levels of a small window (3 CpG sites) of NY-ESO-1. Mean methylation levels \pm standard deviation (SD) were $86.3\% \pm 5.5\%$, $93.3\% \pm 0.6\%$ and $93.3\% \pm 1.5\%$, for U251, T98 and NNS-10 glioma cells, respectively, while it was $30\% \pm 12\%$ for SaOS2 cells constitutively expressing NY-ESO-1. Following 5-aza-CdR treatment, methylation levels were significantly decreased to $54\% \pm 9.1\%$, $68\% \pm 6.9\%$ and $46.7\% \pm 5.7\%$ for U251, T98 and NNS-10 ($p < 0.05$) (Fig. 3c). The MSP and Pyrosequencing data of other glioma cell lines and primary glioma cells were almost identical (data not shown). Taken together, this result is consistent with the hypothesis that 5-aza-CdR mediated NY-ESO-1 activation is a consequence of DNA demethylation.

Upregulation of HLA class I in glioma cells

Our microarray data (supplemental data and Discussion) indicated that HLA class I molecules can be upregulated by ~ 3 -fold (Table SII). Flow cytometric analysis confirmed that HLA class I expression was significantly increased in the 5-aza-CdR-treated glioma cells when compared to that in the untreated cells, indicating that 5-aza-CdR could affect the constitutive expression of HLA class I antigens in gliomas. The representative data of U251 cells are shown in Figure 4a. Combined with the analyses on the effect of 5-aza-CdR on NY-ESO-1 expression, our study suggests that 5-aza-CdR may have potential therapeutic implications in NY-ESO-1-specific immunotherapy for human gliomas.

Antigenicity of forcibly expressed NY-ESO-1 in glioma cells by 5-aza-CdR

To evaluate the antigenicity of forcibly expressed NY-ESO-1, HLA-A2-restricted NY-ESO-1-specific CTL lines were generated, and their cytotoxicity against 5-aza-CdR-treated glioma cells was tested. Cytotoxic activity was observed only in SaOS-2 osteosarcoma cells (NY-ESO-1⁺ and HLA-A2) and 5-aza-CdR-treated U251 glioma cells, depending on the E:T ratios (Fig. 4b). In contrast, untreated U251 cells and other glioma cells (NY-ESO-1⁻ negative and HLA-A2-negative) were resistant to lysis. K562 cells were included in order to assess the degree of the natural-killer activity of the CTL cultures; this activity was found to be negligible. Cold target inhibition assays demonstrated that cytotoxicity against 5-aza-CdR-treated U251 cells was specifically inhibited in the presence of T2.A2 cells that were prepulsed with the cognate but not those that were prepulsed with an irrelevant peptide (Fig. 4c). This indicated that CTL lines recognized the NY-ESO-1 pep-

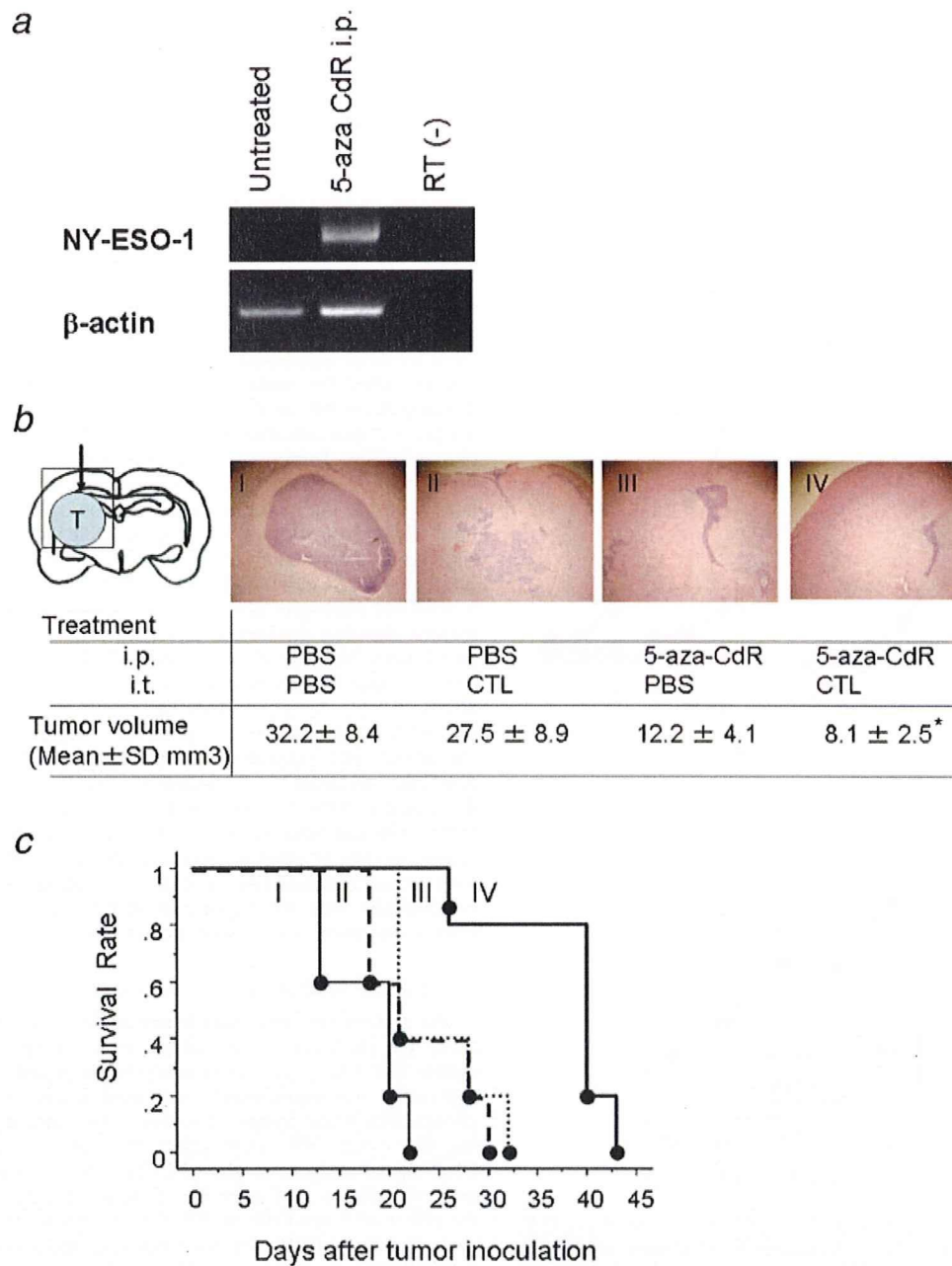


FIGURE 5 – Therapeutic effects of the adoptive transfer of NY-ESO-1-specific CTLs and 5-aza-CdR treatment in the human glioma orthotopic xenograft model. (a) RT-PCR for NY-ESO-1 in intracerebral glioma after i.p. injection of 5-aza-CdR. (b) Histopathological characteristics (haematoxylin and eosin, magnification: 40×) and tumor volumes of animals treated with PBS i.p. (8 pulses from the day after tumor inoculation) and PBS (2 μl) i.t. 6 days after tumor inoculation (Group I), PBS i.p. (8 pulses) and NY-ESO-1-specific bulk CTLs (1 × 10⁶ cells/mouse in 2 μl) i.t. (Group II), 5-aza-CdR i.p. (0.2 mg/kg, 8 pulses) and PBS (2 μl) i.t. (Group III), or 5-aza-CdR i.p. (0.2 mg/kg, 8 pulses) and NY-ESO-1-specific bulk CTLs (1 × 10⁶ cells/mouse in 2 μl) i.t. (Group IV). The mean tumor volume + SD in each group is shown in the table. The schema of brain coronal section shows the tumor (T), the injection site of CTL/PBS (arrow), and the magnified area (box). * $p < 0.05$ compared to other 3 treatment groups. (c) Kaplan–Meier survival curves of groups I–IV. The survival time of mice treated with 5-aza-CdR and NY-ESO-1-specific CTLs was significantly greater than that of mice in Groups I, II and III ($p = 0.0019, 0.0126$ and 0.0132 , respectively).

tides that were processed and presented. These results together indicated that the amount of 5-aza-CdR-induced NY-ESO-1 in glioma cells was sufficient to render them sensitive to HLA-A2-restricted NY-ESO-1-specific CTLs *in vitro*.

Induction of NY-ESO-1 expression in intracerebral glioma by systemic administration of 5-aza-CdR

Previous evidence indicates that 5-aza-CdR can cross the BBB effectively, maintaining cytotoxic concentrations in the cerebro-

spinal fluid when administered *via* continuous intravenous infusion.⁴⁶ To evaluate whether NY-ESO-1 expression could be induced *in vivo* after systemic delivery of 5-aza-CdR, we employed NOD/SCID mice transplanted intracerebrally with U251 glioma cells (NY-ESO-1 negative). After the mice were injected i.p. with a 0.2 mg/kg dose of 5-aza-CdR at 12 hr intervals for 4 days, the tumors were resected and subjected to RT-PCR analysis for NY-ESO-1. The results demonstrated that NY-ESO-1 expression could be detected in intracerebral gliomas i.p. treated with 5-aza-CdR (Fig. 5a).

Growth suppression of glioblastoma xenografts after the adoptive transfer of anti-NY-ESO-1 CTLs

Next, we addressed whether adoptively transferred NY-ESO-1-specific CTLs possess cytotoxic activity against gliomas in which NY-ESO-1 was induced *in vivo* by 5-aza-CdR. In this model, U251 tumor cells were stereotactically implanted in the forebrain of NOD/SCID animals. An intraperitoneal injection of 5-aza-CdR (or PBS) was initiated from the next day for 4 consecutive days at 12-hr intervals. On day 6 after the tumor inoculation, the mice were treated by stereotactic delivery of either NY-ESO-1-specific bulk CTLs or PBS. On day 21 after the tumor inoculation, tumor volumes were evaluated in half of the animals. Tumor growth was significantly delayed in the animals that were administered both 5-aza-CdR (i.p.) and CTLs (Group IV), whereas relatively larger tumors were observed in the other 3 groups (Groups I, II and III, $p < 0.05$) (Fig. 5b). In addition, we measured the survival of the remaining half of the animals. The Kaplan–Meier survival curves of 4 groups are shown in Figure 5c. The survival time of mice treated with 5-aza-CdR and NY-ESO-1-specific CTLs was significantly greater than that of mice in Groups I, II and III ($p = 0.0019, 0.0126$ and 0.0132 , respectively). Interestingly, 5-aza-CdR injection alone (Group III) exerted a beneficial antitumor effect in terms of tumor volumes and survival ($p < 0.05$ vs. Group I). As discussed later, the formation of enzyme-DNA adducts mediated by p53 induction may account for the efficacy and toxicity of 5-aza-CdR *in vivo*.

Discussion

The principal findings of this study are that in spite of relatively low frequency of CTA expression in gliomas, the DNA demethylating agent 5-aza-CdR remarkably induced the expression of CTAs, including NY-ESO-1—one of the most immunogenic CTAs in glioma cells but not in normal human cells. The *de novo* expressed NY-ESO-1 was effectively recognized by the specific CTL lines both *in vitro* and in glioma orthotopic xenografts.

Expression of CTAs in human gliomas

A German group investigated the expression of 7 CTAs (SSX-1, SSX-2, SSX-4, SCP-1, TS85, NY-ESO-1 and MAGE-3) in 50 gliomas by RT-PCR. They demonstrated that SCP-1 was most frequently positive (40%), followed by SSX-4 (27%) and MAGE-3 (7%).³⁵ However, the expression frequency of CTAs in gliomas remains unclear, particularly when focusing on different ethnic groups. For example, NY-ESO-1 and LAGE-1 are expressed at much lower frequencies in lung cancer in the Japanese than in Caucasians; NY-ESO-1 is expressed in 2% of the Japanese versus 17 or 20% in Caucasians, and LAGE-1 is expressed in 9% of the Japanese versus 33% expression in Caucasians.³⁹ Liu *et al.*, have reported MAGE-1 expression in approximately 40% of glioblastoma primary cell lines and in established glioma cell lines, including U87MG, which is inconsistent with our results.⁴⁷ Although the reasons for the inconsistency remain unclear, the differences in ethnic groups and culture conditions (*e.g.*, passage and confluency) might be responsible. Nevertheless, overall, we found that gliomas have a very low frequency of CTA gene expression, such as NY-ESO-1, indicating that brain tumors are considerably unsuitable for CTA-based immunotherapy. To overcome this limitation, novel CTA induction strategies are required to evoke strong immune responses against gliomas.

CTA as targets of demethylation

A cascade of biochemical events for gene silencing is triggered by CpG island methylation that involves DNA methyltransferase activity, which in turn attracts histone deacetylases and histone methylases that eventually modify histones into a silenced chromatin state.⁴⁸ The agent 5-aza-CdR has been shown to interrupt this silencing cascade effectively by binding covalently to DNA methyltransferase and inhibiting its enzymatic activity. Numerous

studies have shown the ability of 5-aza-CdR to reactivate the transcription of several tumor suppressor genes (*i.e.* p16 and MGMT) in human tumors.^{28,29} Previous evidence has clearly defined the regulatory role of DNA methylation in the constitutive expression of CTAs in melanomas and renal cell carcinomas and has demonstrated that *in vitro* treatment with 5-aza-CdR induces their expression in neoplastic cells. Therefore, CTAs are intriguing targets for demethylation. Here, we studied a large panel of CTAs and showed that 5-aza-CdR reactivated the expression of a variety of CTAs in human gliomas. This result is consistent with the report of Liu *et al.*, showing that 5-aza-CdR induced the mRNA expression of MAGE-1.⁴⁷ Then, we determined whether 5-aza-CdR-mediated NY-ESO-1 activation is a consequence of promoter DNA methylation by using MSP and quantitative Pyrosequencing. Although MSP is very sensitive and easy to use, it does not provide precise information about the methylation status of single CpG sites. Recently, Pyrosequencing technology was developed for the analysis of single-base variations. An indirect bioluminescent assay quantitatively measures the amount of pyrophosphate (Ppi) that is released from each incorporated dNTP. Through an enzymatic cascade, the release is converted into a light signal that is directly proportional to the amount of incorporated dNTP, appearing as peaks in a Pyrogram. Employing this technology, we first showed that only a small region of the NY-ESO-1 CpG island provides relevant information for differential methylation analysis.

Expression profiling and gene ontology analysis after 5-aza-CdR treatment

To identify alterations in gene expression after 5-aza-CdR treatment, we conducted microarray experiments (supplementary data). Once the analysis was completed, we narrowed down the number of potential targets by selecting only those genes whose expression changed more than 2-fold in 2 independent RNA preparations. A total of 65 genes that fulfilled our criteria were upregulated, and 24 genes were downregulated following 5-aza-CdR treatment (Table SII). To identify the biological processes significantly involved in the drug effect, genes considered differentially expressed between the treated and control glioma cells were processed through the Gene Ontology (GO) program. The majority of the differentially expressed genes were related to biological process categories such as apoptosis (programmed cell death), cell proliferation, immune system process and tissue development (Table SIII). These categorized GO terms supported the fact that DNA methylation is associated with various biological epigenetic processes, including cell differentiation, development and oncogenic transformation. For the 11 upregulated genes underlined in Supplementary Table SII, we confirmed the microarray data using semiquantitative RT-PCR with the primers listed in Supplementary Table SIV on the same glioma cell line (U251) and 3 others (AO2, T98 and SKMG1). As shown in Supplementary Figure S1, we were able to show marked up-regulation of the tissue inhibitor of metalloprotease (TIMP) gene, which has been found to be silenced by aberrant promoter hypermethylation in other tumor types,⁴⁹ thus validating our screening procedures. Interestingly, p53, Gadd45, NF- κ B and caspase 4 genes were activated by 5-aza-CdR, although the dose of 5-aza-CdR in this study (1 μ M) did not affect the cell viability and morphology in glioma cells (data not shown). Recently, Kim *et al.*, attempted to identify genes silenced epigenetically in malignant gliomas by using a comprehensive and intense microarray technique coupled with the inhibition of DNA methylation and histone deacetylation.⁵⁰ Although they validated the reactivation of the MAGE genes in their microarray screen, they mainly focused on novel targets harbouring the CpG island promoter. In addition to the role of 5-aza-CdR in the activation of epigenetically silenced genes, an important biological activity of this agent is the formation of enzyme-DNA adducts.⁵¹ Karpf *et al.*, reported that the formation of covalent enzyme-DNA adducts and cellular toxicity resulted from the activation of p53 as a cellular response to DNA damage.⁵²

5-Aza-CdR as a potent immunostimulator

Our microarray data (Supplementary data) and the flow cytometric analysis showed that HLA class I expression was significantly increased in the 5-aza-CdR-treated glioma cells. In addition, the efficient recognition of 5-aza-CdR-treated U251 glioma cells by the HLA-A2 restricted NY-ESO-1 specific CTL lines demonstrated that *de novo* synthesized NY-ESO-1 antigen is functionally processed and presented. Thus, CTL-mediated lysis of glioma cells induced by 5-aza-CdR appears to represent a direct consequence of immunogenic peptides derived from *de novo* expressed NY-ESO-1 and loaded onto upregulated HLA class I molecules. Our *in vivo* study suggested that systemic administration of 5-aza-CdR may be useful in reverting the CTA-negative

phenotype of gliomas through the Blood-Brain-Barrier. This evidence strongly identifies 5-aza-CdR as a potential pharmacological agent in designing and establishing new therapeutic strategies in combination with CTA-based immunotherapeutic approaches for glioma patients.

Acknowledgements

The authors thank Mr. Shigeru Saito (Infocom Corporation, Tokyo, Japan) for bioinformatics assistance in Gene Ontology analysis. They also thank Mr. Mitsuo Kihira (Division of Pathology, Kariya Toyota General Hospital, Aichi, Japan) for assistance in the histological study.

References

- Chen YT, Scanlan MJ, Sahin U, Tureci O, Gure AO, Tsang S, Williamson B, Stockert E, Pfreundschuh M, Old LJ. A testicular antigen aberrantly expressed in human cancers detected by autologous antibody screening. *Proc Natl Acad Sci USA* 1997;94:1914-18.
- Boon T, Cerottini JC, Van den Eynde B, van der Bruggen P, Van Pel A. Tumor antigens recognized by T lymphocytes. *Annu Rev Immunol* 1994;12:337-65.
- van der Bruggen P, Traversari C, Chomez P, Lurquin C, De Plaen E, Van den Eynde B, Knuth A, Boon T. A gene encoding an antigen recognized by cytolytic T lymphocytes on a human melanoma. *Science* 1991;254:1643-7.
- Gure AO, Tureci O, Sahin U, Tsang S, Scanlan MJ, Jager E, Knuth A, Pfreundschuh M, Old LJ, Chen YT. SSX: a multigene family with several members transcribed in normal testis and human cancer. *Int J Cancer* 1997;72:965-71.
- Jager D, Unkelbach M, Frei C, Bert F, Scanlan MJ, Jager E, Old LJ, Chen YT, Knuth A. Identification of tumor-restricted antigens NY-BR-1, SCP-1, and a new cancer/testis-like antigen, NW-BR-3 by serological screening of a testicular library with breast cancer serum. *Cancer Immunol* 2002;2:5.
- Hubank M, Schatz DG. Identifying differences in mRNA expression by representational difference analysis of cDNA. *Nucleic Acids Res* 1994;22:5640-8.
- Brinkmann U, Vasmatzis G, Lee B, Yerushalmi N, Essand M, Pastan I. PAGE-1, an X chromosome-linked GAGE-like gene that is expressed in normal and neoplastic prostate, testis, and uterus. *Proc Natl Acad Sci USA* 1998;95:10757-62.
- Lucas S, De Plaen E, Boon T. MAGE-B5, MAGE-B6, MAGE-C2, and MAGE-C3: four new members of the MAGE family with tumor-specific expression. *Int J Cancer* 2000;87:55-60.
- Scanlan MJ, Altorki NK, Gure AO, Williamson B, Jungbluth A, Chen YT, Old LJ. Expression of cancer-testis antigens in lung cancer: definition of bromodomain testis-specific gene (BRDT) as a new CT gene. *Cancer Lett* 2000;150:155-64.
- Jager E, Nagata Y, Gnjatic S, Wada H, Stockert E, Karbach J, Dunbar PR, Lee SY, Jungbluth A, Jager D, Arand M, Ritter G, et al. Monitoring CD8 T cell responses to NY-ESO-1: correlation of humoral and cellular immune responses. *Proc Natl Acad Sci USA* 2000;97:4760-5.
- Choi JH, Kwon HJ, Yoon BI, Kim JH, Han SU, Joo HJ, Kim DY. Expression profile of histone deacetylase 1 in gastric cancer tissues. *Jpn J Cancer Res* 2001;92:1300-4.
- Jones PA, Takai D. The role of DNA methylation in mammalian epigenetics. *Science* 2001;293:1068-70.
- Jones PA, Baylin SB. The fundamental role of epigenetic events in cancer. *Nat Rev Genet* 2002;3:415-28.
- Eden A, Gaudet F, Waghmare A, Jaenisch R. Chromosomal instability and tumors promoted by DNA hypomethylation. *Science* 2003;300:455.
- Gaudet F, Hodgson JG, Eden A, Jackson-Grusby L, Dausman J, Gray JW, Leonhardt H, Jaenisch R. Induction of tumors in mice by genomic hypomethylation. *Science* 2003;300:489-92.
- Bariol C, Suter C, Cheong K, Ku SL, Meagher A, Hawkins N, Ward R. The relationship between hypomethylation and CpG island methylation in colorectal neoplasia. *Am J Pathol* 2003;162:1361-71.
- Lin CH, Hsieh SY, Sheen IS, Lee WC, Chen TC, Shyu WC, Liaw YF. Genome-wide hypomethylation in hepatocellular carcinogenesis. *Cancer Res* 2001;61:4238-43.
- Narayan A, Ji W, Zhang XY, Marrogi A, Graff JR, Baylin SB, Ehrlich M. Hypomethylation of pericentromeric DNA in breast adenocarcinomas. *Int J Cancer* 1998;77:833-8.
- dos Santos NR, Torensma R, de Vries TJ, Schreurs MW, de Bruijn DR, Kater-Baats E, Rutter DJ, Adema GJ, van Muijen GN, van Kessel AG. Heterogeneous expression of the SSX cancer/testis antigens in human melanoma lesions and cell lines. *Cancer Res* 2000;60:1654-62.
- Missiaglia E, Donadelli M, Palmieri M, Crnogorac-Jurcevic T, Scarpa A, Lemoine NR. Growth delay of human pancreatic cancer cells by methylase inhibitor 5-aza-2'-deoxycytidine treatment is associated with activation of the interferon signalling pathway. *Oncogene* 2005;24:199-211.
- Mompalmer RL, Ayoub J. Potential of 5-aza-2'-deoxycytidine (Decitabine) a potent inhibitor of DNA methylation for therapy of advanced non-small cell lung cancer. *Lung Cancer* 2001;34(Suppl 4):S111-S115.
- Jackson-Grusby L, Laird PW, Magge SN, Moeller BJ, Jaenisch R. Mutagenicity of 5-aza-2'-deoxycytidine is mediated by the mammalian DNA methyltransferase. *Proc Natl Acad Sci USA* 1997;94:4681-5.
- Santi DV, Norment A, Garrett CE. Covalent bond formation between a DNA-cytosine methyltransferase and DNA containing 5-azacytosine. *Proc Natl Acad Sci USA* 1984;81:6993-7.
- Santini V, Kantarjian HM, Issa JP. Changes in DNA methylation in neoplasia: pathophysiology and therapeutic implications. *Ann Intern Med* 2001;134:573-86.
- Samlowski WE, Leachman SA, Wade M, Cassidy P, Porter-Gill P, Busby L, Wheeler R, Boucher K, Fitzpatrick F, Jones DA, Karpf AR. Evaluation of a 7-day continuous intravenous infusion of decitabine: inhibition of promoter-specific and global genomic DNA methylation. *J Clin Oncol* 2005;23:3897-905.
- Wijermans P, Lubbert M, Verhoef G, Bosly A, Ravooet C, Andre M, Ferrant A. Low-dose 5-aza-2'-deoxycytidine, a DNA hypomethylating agent, for the treatment of high-risk myelodysplastic syndrome: a multicenter phase II study in elderly patients. *J Clin Oncol* 2000;18:956-62.
- Kantarjian H, Issa JP, Rosenfeld CS, Bennett JM, Albitar M, DiPersio J, Klimek V, Slack J, de Castro C, Ravandi F, Helmer R, III, Shen L, et al. Decitabine improves patient outcomes in myelodysplastic syndromes: results of a phase III randomized study. *Cancer* 2006;106:1794-803.
- Coral S, Sigalotti L, Altomonte M, Engelsberg A, Colizzi F, Cattarossi I, Maraskovsky E, Jager E, Seliger B, Maio M. 5-aza-2'-deoxycytidine-induced expression of functional cancer testis antigens in human renal cell carcinoma: immunotherapeutic implications. *Clin Cancer Res* 2002;8:2690-5.
- Coral S, Sigalotti L, Gasparollo A, Cattarossi I, Visintin A, Cattelan A, Altomonte M, Maio M. Prolonged upregulation of the expression of HLA class I antigens and costimulatory molecules on melanoma cells treated with 5-aza-2'-deoxycytidine (5-AZA-CdR). *J Immunother* 1999;22:16-24.
- Schwechheimer K, Lauffle RM, Schmah W, Knodlseder M, Fischer H, Hofler H. Expression of neu/c-erbB-2 in human brain tumors. *Hum Pathol* 1994;25:772-80.
- Hiesiger EM, Hayes RL, Pierz DM, Budzilovich GN. Prognostic relevance of epidermal growth factor receptor (EGF-R) and c-neu/erbB2 expression in glioblastomas (GBMs). *J Neurooncol* 1993;16:93-104.
- Chi DD, Merchant RE, Rand R, Conrad AJ, Garrison D, Turner R, Morton DL, Hoon DS. Molecular detection of tumor-associated antigens shared by human cutaneous melanomas and gliomas. *Am J Pathol* 1997;150:2143-52.
- Scarcella DL, Chow CW, Gonzales MF, Economou C, Brasseur F, Ashley DM. Expression of MAGE and GAGE in high-grade brain tumors: a potential target for specific immunotherapy and diagnostic markers. *Clin Cancer Res* 1999;5:335-41.
- Rimoldi D, Romero P, Carrel S. The human melanoma antigen-encoding gene, MAGE-1, is expressed by other tumour cells of neuroectodermal origin such as glioblastomas and neuroblastomas. *Int J Cancer* 1993;54:527-8.
- Sahin U, Koslowski M, Tureci O, Eberle T, Zwick C, Romeike B, Moringlane JR, Schwechheimer K, Feiden W, Pfreundschuh M. Expression of cancer testis genes in human brain tumors. *Clin Cancer Res* 2000;6:3916-22.

36. Debinski W, Gibo DM, Hulet SW, Connor JR, Gillespie GY. Receptor for interleukin 13 is a marker and therapeutic target for human high-grade gliomas. *Clin Cancer Res* 1999;5:985-90.
37. Okano F, Storkus WJ, Chambers WH, Pollack IF, Okada H. Identification of a novel HLA-A*0201-restricted, cytotoxic T lymphocyte epitope in a human glioma-associated antigen, interleukin 13 receptor α 2 chain. *Clin Cancer Res* 2002;8:2851-5.
38. Jager E, Chen YT, Drijfhout JW, Karbach J, Ringhoffer M, Jager D, Arand M, Wada H, Noguchi Y, Stockert E, Old LJ, Knuth A. Simultaneous humoral and cellular immune response against cancer-testis antigen NY-ESO-1: definition of human histocompatibility leukocyte antigen (HLA)-A2-binding peptide epitopes. *J Exp Med* 1998;187:265-70.
39. Tajima K, Obata Y, Tamaki H, Yoshida M, Chen YT, Scanlan MJ, Old LJ, Kuwano H, Takahashi T, Takahashi T, Mitsudomi T. Expression of cancer/testis (CT) antigens in lung cancer. *Lung Cancer* 2003;42:23-33.
40. Herman JG, Graff JR, Myohanen S, Nelkin BD, Baylin SB. Methylation-specific PCR: a novel PCR assay for methylation status of CpG islands. *Proc Natl Acad Sci USA* 1996;93:9821-6.
41. Colella S, Shen L, Baggerly KA, Issa JP, Krahe R. Sensitive and quantitative universal Pyrosequencing methylation analysis of CpG sites. *Biotechniques* 2003;35:146-50.
42. Gardiner-Garden M, Frommer M. CpG islands in vertebrate genomes. *J Mol Biol* 1987;196:261-82.
43. Natsume A, Ishii D, Wakabayashi T, Tsuno T, Hatano H, Mizuno M, Yoshida J. IFN- β down-regulates the expression of DNA repair gene MGMT and sensitizes resistant glioma cells to temozolomide. *Cancer Res* 2005;65:7573-9.
44. James SR, Link PA, Karpf AR. Epigenetic regulation of X-linked cancer/germline antigen genes by DNMT1 and DNMT3b. *Oncogene* 2006;25:6975-85.
45. Arai J, Yasukawa M, Ohminami H, Kakimoto M, Hasegawa A, Fujita S. Identification of human telomerase reverse transcriptase-derived peptides that induce HLA-A24-restricted antileukemia cytotoxic T lymphocytes. *Blood* 2001;97:2903-7.
46. Chabot GG, Rivard GE, Momparler RL. Plasma and cerebrospinal fluid pharmacokinetics of 5-Aza-2'-deoxycytidine in rabbits and dogs. *Cancer Res* 1983;43:592-7.
47. Liu G, Ying H, Zeng G, Wheeler CJ, Black KL, Yu JS. HER-2, gp100, and MAGE-1 are expressed in human glioblastoma and recognized by cytotoxic T cells. *Cancer Res* 2004;64:4980-6.
48. Jaenisch R, Bird A. Epigenetic regulation of gene expression: how the genome integrates intrinsic and environmental signals. *Nat Genet* 2003;33(Suppl):245-54.
49. Ivanova T, Vinokurova S, Petrenko A, Eshilev E, Solovyova N, Kissel'jov F, Kissel'jova N. Frequent hypermethylation of 5' flanking region of TIMP-2 gene in cervical cancer. *Int J Cancer* 2004;108:882-6.
50. Kim TY, Zhong S, Fields CR, Kim JH, Robertson KD. Epigenomic profiling reveals novel and frequent targets of aberrant DNA methylation-mediated silencing in malignant glioma. *Cancer Res* 2006;66:7490-501.
51. Ferguson AT, Vertino PM, Spitzner JR, Baylin SB, Muller MT, Davidson NE. Role of estrogen receptor gene demethylation and DNA methyltransferase-DNA adduct formation in 5-aza-2'-deoxycytidine-induced cytotoxicity in human breast cancer cells. *J Biol Chem* 1997;272:32260-6.
52. Karpf AR, Moore BC, Ririe TO, Jones DA. Activation of the p53 DNA damage response pathway after inhibition of DNA methyltransferase by 5-aza-2'-deoxycytidine. *Mol Pharmacol* 2001;59:751-7.